

1  
2 1  
3 2  
4 3  
5 4  
6 5  
7 6  
8 7  
9 8  
10 9  
11 10  
12 11  
13 12  
14 13  
15 14  
16 15  
17 16  
18 17  
19 18  
20 19  
21 20  
22 21  
23 22  
24 23  
25 24  
26 25  
27 26  
28 27  
29 28  
30 29  
31 30  
32 31  
33 32  
34 33  
35 34  
36 35  
37 36  
38 37  
39 38  
40 39  
41 40  
42 41  
43 42  
44 43  
45 44  
46 45  
47 46  
48 47  
49 48  
50 49  
51 50  
52 51  
53 52  
54 53  
55 54  
56 55  
57 56  
58 57  
59 58  
60 59

**A putative structural variant and environmental variation associated with genomic divergence across the Northwest Atlantic in Atlantic Halibut**

Tony Kess<sup>1\*</sup>, Anthony L. Einfeldt<sup>2</sup>, Brendan Wringe<sup>3</sup>, Sarah J. Lehnert<sup>1</sup>, Kara K. S. Layton<sup>4</sup>, Meghan C. McBride<sup>3</sup>, Dominique Robert<sup>5</sup>, Jonathan Fisher<sup>6</sup>, Arnault Le Bris<sup>6</sup>, Cornelia den Heyer<sup>3</sup>, Nancy Shackell<sup>3</sup>, Daniel Ruzzante<sup>2</sup>, Paul Bentzen<sup>2</sup>, Ian R. Bradbury<sup>1</sup>

1. Fisheries and Oceans Canada, Northwest Atlantic Fisheries Centre, St. John's, NL, Canada

2. Biology Department, Dalhousie University, Halifax, NS, Canada

3. Fisheries and Oceans Canada, Bedford Institute of Oceanography, Dartmouth, NS, Canada

4. School of Biological Sciences, University of Aberdeen, Aberdeen, Scotland, UK

5. Institut des sciences de la mer de Rimouski, Université du Québec à Rimouski, Rimouski, QC, Canada

6. Centre for Fisheries Ecosystems Research, Fisheries and Marine Institute of Memorial University of Newfoundland, St. John's, NL, Canada

\*Corresponding author: Tony Kess, [tony.kess@dfo-mpo.gc.ca](mailto:tony.kess@dfo-mpo.gc.ca)

**Abstract**

Characterizing the nature of genetic differentiation among individuals and populations and its distribution across the genome is increasingly important to inform both conservation and management of exploited species. Atlantic Halibut (*Hippoglossus hippoglossus*) is an ecologically and commercially important fish species, yet knowledge of population structure and genomic diversity in this species remains lacking. Here, we use restriction-site associated DNA sequencing and a chromosome-level genome assembly to identify over 86,000 single nucleotide polymorphisms mapped to 24 chromosome-sized scaffolds, genotyped in 734 individuals across the Northwest Atlantic. We describe subtle but significant genome-wide regional structuring between the Gulf of St. Lawrence and adjacent Atlantic continental shelf. However, the majority of genetic divergence is associated with a large putative chromosomal rearrangement (5.74 megabases) displaying high differentiation and linkage disequilibrium, but no evidence of geographic variation. Demographic reconstructions suggest periods of expansion coinciding with glacial retreat, and more recent declines in  $N_e$ . This work highlights the utility of genomic data to identify multiple sources of genetic structure and genomic diversity in commercially exploited marine species.

## 55 Introduction

56  
57 Identifying the genomic basis of population structure and local adaptation is a fundamental goal  
58 of both evolutionary biology (Savolainen *et al.*, 2013) and conservation genetics (Funk *et al.*, 2012),  
59 and is key to delineating and conserving intraspecific diversity. Detecting this variation in marine  
60 species has been challenging due to low levels of differentiation, large population sizes, and high  
61 connectivity frequently uncovered in marine organisms, which have often precluded the resolution of  
62 significant population divergence using neutral genetic markers (Hauser and Carvalho 2008; Gagnaire  
63 *et al.* 2015). However, with expanded availability of massively parallel sequencing, genomic analyses  
64 of population structure in marine species have increasingly revealed diverse and complex signatures of  
65 population differentiation (Lamichhaney *et al.*, 2012, 2017; Van Wyngaarden *et al.*, 2017). These  
66 patterns range from genome-wide polygenic variation associated with subtle, coordinated shifts in  
67 allele frequency at multiple loci (Le Corre and Kremer 2012; Bay and Palumbi 2014; Babin *et al.* 2017)  
68 to localized genomic regions housing structural variants or genes of large effect within otherwise  
69 undifferentiated genomes (Prince *et al.*, 2017; Kess *et al.*, 2019; Longo *et al.*, 2020). Across studies,  
70 genomic differentiation has been found associated with environmental variation (Bradbury *et al.*, 2010;  
71 Lamichhaney *et al.*, 2012; Stanley *et al.*, 2018), spawning time (Lamichhaney *et al.*, 2017) and  
72 behavioural traits (Prince *et al.*, 2017; Kess *et al.*, 2019). These observations support the hypothesis  
73 that genetic structuring in marine species often underlies adaptive differences that delineate significant  
74 ecological diversity, revealing adaptation at multiple geographic scales. Uncovering the genetic  
75 architecture underlying environmentally-associated and adaptive genetic variation can inform how  
76 distinct populations should be managed and conserved (Funk *et al.*, 2012), and increasingly can enable  
77 examinations of past and future responses to environmental change (Bay *et al.*, 2017; Lehnert *et al.*,  
78 2019; Layton *et al.*, 2021).

79 Recent methodological advances have enabled estimation of demographic history in non-  
80 model species, allowing identification of historical changes that have impacted populations (Barbato *et*  
81 *al.*, 2015; Liu and Fu 2015; Hollenbeck *et al.*, 2016). Observations from these studies have uncovered  
82 correspondence between climate shifts or potential human impacts, and perturbations to species  
83 demographic histories (Cristofari *et al.*, 2018; Vijay *et al.*, 2018; Lehnert *et al.*, 2019). Past changes in  
84 demography can have far-reaching impacts on contemporary diversity and shed light on factors shaping  
85 adaptive variation within species (Mitchell-Olds *et al.*, 2007; Ellegren and Galtier 2016). Pairing  
86 estimates of genetic diversity with demographic reconstruction methods can reveal how historical

1  
2 87 forces have shaped the diversity of contemporary populations and can further aid in understanding the  
3  
4 88 adaptive potential of studied species (Ruzzante *et al.*, 2008; Wang *et al.*, 2017).

5 89 Atlantic Halibut (*Hippoglossus hippoglossus*), a migratory, cold-water, and economically  
6  
7 90 valuable groundfish species (DFO 2018), is currently managed in Canada as two distinct stocks: one  
8  
9 91 stock on the Atlantic continental shelf, spanning the Scotian Shelf and the southern Grand Banks in  
10  
11 92 NAFO divisions 3NOPs4VWX5Zc, and a second in the Gulf of St. Lawrence spanning NAFO  
12  
13 93 divisions 4RST (DFO 2015a, 2015b). There is significant heterogeneity in stock status across the  
14  
15 94 northwest Atlantic, with recent and historical examples of population decline in US stocks contrasting  
16  
17 95 dramatic increases in Canadian waters (Grasso 2008; Shackell *et al.* 2016; Trzcinski and Bowen 2016).  
18  
19 96 Despite its commercial and ecological importance, there is little understanding of how existing  
20  
21 97 management units correspond to genomic differentiation or adaptive diversity within this species.  
22  
23 98 Atlantic Halibut exhibit regional differences in life history, suggesting the potential for cryptic fine-  
24  
25 99 scale genetic differentiation among populations across the Northwest Atlantic (Armsworthy and  
26  
27 100 Campana 2010; Shackell *et al.*, 2019) but any genetic basis for these differences remains unknown,  
28  
29 101 with essentially no population structure detected using microsatellite loci (e.g., Reid *et al.*, 2005). The  
30  
31 102 genomic consequences of demographic change, and the level of contemporary diversity in Atlantic  
32  
33 103 halibut populations also remains unknown, limiting understanding of how this species has responded to  
34  
35 104 past disturbance or could respond in the future to ongoing climate change. Genomic methods have the  
36  
37 105 capacity to reveal cryptic structure in exploited marine species (Selkoe *et al.*, 2016; Kelley *et al.*,  
38  
39 106 2016), and application of genomic tools to quantify population structure is integral to informing the  
40  
41 107 conservation and management of Atlantic Halibut in the Northwest Atlantic.

42 108 In this study, we use genome-wide single nucleotide polymorphisms (SNP) obtained by  
43  
44 109 restriction-site associated DNA (RAD) sequencing (Baird *et al.*, 2008) to investigate population  
45  
46 110 genomic structure, diversity, and demographic history in Atlantic Halibut sampled across the  
47  
48 111 Northwest Atlantic. Specifically, we (1) examine population structure across the Northwest Atlantic,  
49  
50 112 and quantify divergence associated with a large putative chromosomal rearrangement, newly identified  
51  
52 113 in this study, (2) explore the presence of environmental associations with population structure across  
53  
54 114 the Northwest Atlantic, potentially indicative of adaptation, and (3) reconstruct the demographic  
55  
56 115 history of Atlantic Halibut over the past 150,000 years and explore temporal associations with climate.  
57  
58 116 Our findings here support a role for environmental variability in shaping genetic diversity in marine  
59  
60 117 species, and provides empirical support for subtle genome-wide divergence in the marine environment.

## 120 **Methods**

### 122 **Sampling & Sequencing**

123 We obtained tissue samples from Atlantic Halibut caught between 2017 and 2018 on  
124 Department of Fisheries and Oceans (DFO) Canada trawl surveys, DFO-Industry longline surveys,  
125 Maine Department of Marine Resources trawl surveys, Nature Conservancy-Cape Cod industry  
126 samples, and Spanish Institute of Oceanography surveys in NAFO regions outside the Canadian  
127 Exclusive Economic Zone in NAFO Divs. 3N, 3O, and on the Flemish Cap (See Table 1 for location  
128 and sampling details) distributed across the Northwest Atlantic (Figure 1). Tissue samples were taken  
129 from fin clips, hearts, or spleens of sampled fish, and preserved in 95% ethanol. Sex was inferred from  
130 the visual identification of reproductive organs during dissection of sampled fish.

131 DNA was extracted from tissue samples using Qiagen QIAamp 96 DNA QIAcube HT Kit and  
132 QIAamp DNA Mini Kit extraction kits and assessed for DNA quality using Quant-iT PicoGreen.  
133 Following DNA extraction, RADseq libraries were constructed from 768 individual tissue samples  
134 passing DNA quality thresholds. Libraries were developed following an adapted and optimized version  
135 of the Ali *et al.*, 2016 protocol without the use of bait sequences to recover specific genomic regions,  
136 following the method described as “New RAD” in the initial publication and referred to as “bestRAD”  
137 in subsequent studies (e.g. Rochette et al. 2019). For each library, we randomized 48 individuals across  
138 regions, digested DNA using the *SbfI* restriction enzyme, and then ligated 48 unique RAD-Cap  
139 barcodes to each individual within a library. We then pooled, purified, and sheared DNA from these  
140 uniquely barcoded individuals, followed by isolating sheared RAD-tagged DNA for each pool. Library  
141 preparation then followed NEBNext Ultra DNA Library Prep for Illumina with no modifications. Each  
142 library received a unique index (1-16) which corresponded with the library number (e.g., Library 1 had  
143 index 1). Pooled libraries of 48 uniquely-barcoded individuals were sequenced on 16 separate lanes of  
144 an Illumina HiSeq 4000, using paired end sequencing of 100bp reads, at the McGill University and  
145 Génome Québec Innovation Centre.

### 147 **Read Processing and SNP calling**

148 Read quality for each library was checked using FastQC (Andrews et al. 2010) and we then  
149 used cutadapt 2.1 (Martin 2011) to trim all reads to a minimum length of 90 bp and remove adapter  
150 read-through sequence. Reads were then demultiplexed using the *process\_radtags* function in Stacks  
151 2.5 (Rochette *et al.*, 2019), using the *bestRAD* flag, a barcode distance of 2, and removing reads with  
152 uncalled bases or falling below the default quality score. We then aligned all paired, demultiplexed

reads to the Atlantic Halibut Primary Curated reference genome (Einfeldt *et al.*, *in prep*, available at [https://vgp.github.io/genomeark/Hippoglossus\\_hippoglossus/](https://vgp.github.io/genomeark/Hippoglossus_hippoglossus/)), using the Burrows-Wheeler algorithm in *bwa mem* 0.7.17 (Li 2013), and sorted aligned reads using SAMtools 1.9 (Li *et al.*, 2009). We used *gstacks* in Stacks 2.5 to remove PCR duplicates with the *-rm-pcr-duplicates* flag and call RAD loci and SNPs, and then used *populations* to export a variant call format (vcf) file of SNPs using the *-vcf* flag, filtered for minor allele frequencies of 0.01 (*--min-maf* 0.01) with a minimum genotyping rate of 0.8 (*-r* 80). We then used *vcftools* (Danecek *et al.*, 2011) to remove SNPs not aligned to the 24 large chromosomal scaffolds, or with a minimum depth below 15 reads. We tested SNPs for deviation from Hardy Weinberg equilibrium (HWE) in plink 1.9 (Chang *et al.*, 2015) and calculated false discovery rate *q* values (Storey and Tibshirani 2003) for significant HWE deviation using the R package *qvalue* (Storey 2015). We then removed SNPs in autosomal regions with *q* values less than 0.05 in both the Atlantic continental shelf region as well as in the Gulf of St. Lawrence. Initial population structure analysis with *pcadapt* (Luu *et al.*, 2017) revealed a single large cluster containing the majority of individuals ( $n = 751$ ), and 12 individuals separated on the first four PC axes (Supplementary Figure 1), but a low overall proportion of genetic variation explained ( $< 1\%$ ). We conducted separate Identity By Descent (IBD) analyses in plink using the *genome* function on these 12 individuals and the set of 751 individuals which did not reveal aberrant PCA clustering, and found high pi-hat values ( $> 0.975$ ) among 8 individuals. Comparisons among individuals in this set also showed elevated pi-hat values overall (mean pi-hat = 0.3) relative to the larger dataset of 751 individuals (mean pi-hat = 0.004). Together, these differences in IBD and PCA clustering indicate potential genotyping of duplicate samples, closely related individuals, or those from another lineage (Stevens *et al.*, 2011). These individuals were removed from subsequent analyses ( $n = 12$ ). We then removed individuals that had incomplete sampling information from DFO surveys ( $n = 17$ ). These filtering steps resulted in a final dataset of 86,043 SNPs distributed across the genome in 734 individuals.

To explore the impact of removing linked loci on inference of population structure, we also produced three additional panels of SNPs: 1. by removing chromosomes S15 and S18 due to identification of a putative chromosomal inversion on chromosome S15 (see below) and a sex-associated region on chromosome S18, found by PCA clustering of the initial 86,043 SNPs, which impacted detection of geographic population structure; 2. by filtering for linkage disequilibrium (LD) to generate an LD-pruned panel through removal of SNPs with  $r^2 > 0.5$  in 50 SNP sliding windows, analyzed iteratively in steps of five SNPs using plink, and removing chromosomes S15 and S18; 3. a panel of SNPs with a single SNP per RAD locus retained, and removing S15 and S18. A breakdown of

1  
2 185 the number of SNPs, RAD loci, and proportion of SNPs mapping to each strand orientation at each  
3  
4 186 stage of filtering are provided in Table 2.

## 7 188 **Range-wide Population structure and Genetic differentiation**

8  
9 189 We first examined population structure across the Gulf of St. Lawrence and Atlantic continental  
10  
11 190 shelf using principal component analysis (PCA) in the R package *pcadapt*. We conducted PCA using  
12  
13 191 all SNPs 86,043 SNPs, followed by PCA using each of the subset SNP panels (i.e., filtered for LD and  
14  
15 192 with single SNPs per RAD retained, with chromosomes S15 and S18 removed). We then identified  
16  
17 193 SNPs significantly associated with population structure based on Mahalanobis distance of correlations  
18  
19 194 with  $K = 3$  PC axes, selected based on absence of genetic structure detected on subsequent axes, which  
20  
21 195 instead separated individual samples. We then calculated  $q$  values for each SNP, and selected outliers  
22  
23 196 as those SNPs with significant associations with  $K = 3$  PC axes with  $q < 0.05$ . To test for within-region  
24  
25 197 genetic variation, we conducted PCA using individuals sampled from the Atlantic continental shelf  
26  
27 198 ( $N=521$  individuals) and within the Gulf of St. Lawrence ( $N=213$  individuals) separately, and a set of  
28  
29 199 62,213 SNPs with chromosomes S15 and S18 removed to prioritize detecting spatial structure rather  
30  
31 200 than the putative rearrangement or sex locus.

32  
33 201 We calculated ancestry proportions for each individual using the sparse non-negative matrix  
34  
35 202 factorization (*snmf*) function in the R package *LEA* (Frichot *et al.*, 2014; Frichot and Francois 2015)  
36  
37 203 using the panel of 62,213 SNPs with S15 and S18 removed, to prevent assignment of ancestry to  
38  
39 204 individuals based on putative inversion or sex chromosome variation. We investigated  $K = 1-5$  sources  
40  
41 205 of ancestry, tested for the number of significant sources of genetic ancestry using cross-entropy criteria,  
42  
43 206 and repeated this analysis with the SNP panels filtered for LD, and with a single SNPs per RAD locus  
44  
45 207 retained.

46  
47 208 We calculated Weir and Cockerham's (1984)  $F_{ST}$  in plink between samples obtained from the  
48  
49 209 Gulf of St. Lawrence and the Atlantic continental shelf and assessed significance of  $F_{ST}$  values in the R  
50  
51 210 package *StAMPP* using 500 bootstraps (Pembleton *et al.*, 2013) using the full dataset of 86,043 SNPs.  
52  
53 211 This grouping was selected based on subtle genetic differentiation observed between these regions  
54  
55 212 using *pcadapt*, as well as the current management regime for Atlantic halibut in Canadian waters. To  
56  
57 213 identify SNPs associated with subtle genetic structuring between regions, we selected the top 1% of  
58  
59 214 SNPs based on  $F_{ST}$  as outliers. We then explored the utility of these SNPs in delineating population  
60  
215 structure as a possible method to identify structure despite low overall genomic differentiation  
216 (Gagnaire *et al.* 2015) by repeating *pcadapt* and *snmf* analyses using only  $F_{ST}$  outlier SNPs. Last, to test  
217 for significant differentiation within the Atlantic continental shelf, we compared  $F_{ST}$  between

1  
2 218 individuals from the most distant regions of this sampling area. We estimated  $F_{ST}$  between 60  
3  
4 219 individuals from the Gulf of Maine and 60 individuals from Newfoundland and Grand Banks, and  
5  
6 220 assessed significance using *StAMPP*.

## 7 221 8 9 222 **Environmental association**

10 223 We calculated associations between SNP genotype and environmental variables to identify the  
11 224 role of oceanographic features in driving population structure and genomic differentiation. First, we  
12 224 role of oceanographic features in driving population structure and genomic differentiation. First, we  
13  
14 225 extracted environmental values averaged over all months and years from 2000 to 2014. These  
15  
16 226 variables included maximum, mean, and minimum salinity, dissolved oxygen content, and temperature  
17  
18 227 at mean bottom depth for the sampling location of each individual, obtained from the Bio-Oracle 2.2  
19 228 database (Assis *et al.*, 2018), using the R package *sdmpredictors* (Bosch 2018). To reduce the number  
20  
21 229 of correlated variables tested for environmental association, we standardized each variable by its  
22  
23 230 standard deviation and then conducted principal component analyses separately on temperature,  
24  
25 231 salinity, and oxygen variables to produce three principal components (Supplementary Figure 2). We  
26  
27 232 used the first axis of each principal component as aggregate measures of temperature, salinity, and  
28  
29 233 dissolved oxygen. Pearson's correlation coefficients among each of these PCs were below 0.7 in all  
30  
31 234 pairwise comparisons, and thus we retained all three of these PCs as predictors for environmental  
32  
33 235 association. We then conducted redundancy analysis (RDA, Rao 1964) with the *vegan* R package  
34  
35 236 (Oksanen *et al.*, 2011), using principal components of environmental variables as predictors and SNP  
36  
37 237 genotypes as response variables. We also conducted a partial RDA that was first constrained by latitude  
38  
39 238 and longitude values to assess the role of environment independent of geography in generating genomic  
40  
41 239 differentiation. Last, the significance of geography alone was assessed through an RDA on only  
42  
43 240 geographic coordinates. The significance of each model was assessed using 999 permutations with the  
44  
45 241 *anova.cca* function.

46  
47 242 To identify SNPs significantly associated with environmental variables, we used the *Rdadapt* R  
48  
49 243 function (Capblancq *et al.*, 2018, Supporting Information Script S1) to calculate Mahalanobis distances  
50  
51 244 of z-transformed canonical axis loadings on all three canonical axes, selected based on visualization of  
52  
53 245 Scree plots. This method allows for a statistical test of significance of association of SNPs with  
54  
55 246 environmental variables, by computing per-SNP  $p$  values estimated from Mahalanobis distances for  
56  
57 247 each SNP, which can then be adjusted as  $q$  values for False Discovery Rate. Here, we used a  
58  
59 248 conservative approach to identify outlier SNPs as those with a  $q$  value  $< 0.05$  and canonical axis  
60  
61 249 scores  $>$  the 99.9th percentile of a canonical axis. We then compared the number of environmental  
62  
63 250 outlier SNPs detected from RDA and RDA with constraint by geographic variation.



## Characterization of a potential structural variant

We identified a highly divergent genomic region on chromosome 15 in *pcadapt* comparisons consistent with a potential structural variant. To quantify divergence between different genotypes heterozygous or homozygous for either allele of this genomic region, we separated individuals into genotype groups based on PC1 score from PCA restricted to chromosome 15. We then estimated  $F_{ST}$  between homozygous genotype groups. To quantify linkage disequilibrium (LD), we estimated pairwise  $r^2$  between all SNPs on chromosome 15 in plink and estimated mean  $r^2$  for each SNP with all adjacent SNPs in 50 SNP windows. We then calculated Pearson correlation coefficients for LD ( $r^2$ ) and  $F_{ST}$  for SNPs within and outside of the putative structural variant. Next, we estimated heterozygosity per SNP for each genotype group, as well as LD in 50 SNP windows for each genotype group, and used Mann Whitney U Tests to compare significance of LD and heterozygosity estimates within and outside the putative rearrangement. We then carried out a test of Hardy Weinberg Equilibrium in plink using assigned putative inversion genotypes as a single locus.

We conducted an additional test for the presence of a structural variant on chromosome 15 using the R package *inversion* (Cáceres et al., 2012), which uses patterns of local LD to infer and phase inversion breakpoints, assuming the population consists of both inverted and non-inverted haplotypes, with inversion size inferred from patterns of contiguous LD.

To identify potential molecular functions of this region we extracted annotation information from the coordinates of the divergent region from chromosome NC\_047158.1, which corresponds to S15 in the Primary Curated reference used for SNP calling, in the annotated GCA\_009819705.1 Atlantic Halibut assembly (available at [https://www.ncbi.nlm.nih.gov/assembly/GCA\\_009819705.1](https://www.ncbi.nlm.nih.gov/assembly/GCA_009819705.1)), using the .gff format annotation and using bedtools (Quinlan and Hall 2010). We then extracted all annotated genes with gene symbols from aligned regions, and conducted a gene ontology overrepresentation test of all biological and molecular terms using the *Danio rerio* and *Homo sapiens* genomes for separate comparisons in PANTHER (Mi et al., 2019), using a Bonferroni adjusted alpha of 0.05 for significant terms.

## Genetic diversity and demographic history

We estimated genetic diversity and demographic history separately in Gulf of St. Lawrence and Atlantic samples, based on separate management regimes and genomic differentiation between these sites. We estimated per-locus observed ( $H_o$ ) and expected ( $H_e$ ) heterozygosity using plink. We then randomly chose 60 individuals from each region and downsampled to 1000 un-linked SNPs with minor

1  
2 284 allele frequency  $> 0.05$  to calculate recent effective population size ( $N_e$ ) for each region using  
3  
4 285 NeESTIMATOR v 2.0 (Do *et al.*, 2014).  
5  
6 286 ANGSD 0.931 was used to export folded site-frequency spectra (SFS) for calculation of  
7  
8 287 nucleotide diversity ( $\pi$ ), Tajima's D, and demographic reconstruction in each region. We used the  
9  
10 288 Picard 2.26 *MarkDuplicates* function and *IndelRealigner* function in Genome Analysis Toolkit v3.7.0  
11  
12 289 (DePristo *et al.*, 2011) to generate a set of sorted, indel-realigned, de-duplicated bam alignments for  
13  
14 290 200 individuals from the Atlantic continental shelf and 200 individuals from the Gulf of St. Lawrence.  
15  
16 291 Site frequency spectra for all chromosomes, excluding S15 and S18, were exported for samples from  
17  
18 292 the Gulf of St. Lawrence and from the Atlantic continental shelf separately using ANGSD 0.931  
19  
20 293 (Korneliussen *et al.*, 2014), and the reference genome as the ancestral genome, with the following  
21  
22 294 flags: *-dosaf 1 -minMapQ 30 -minQ 20 -minInd 200 -doMajorMinor 5 -doMaf 2 -uniqueOnly 1 -*  
23  
24 295 *remove\_bads 1 -only\_proper\_pairs 1*. We generated SFS from 13,001,232 and 12,148,475 genotyped  
25  
26 296 variant and invariant sites in the Atlantic continental shelf and Gulf of St. Lawrence samples,  
27  
28 297 respectively. We then output folded site frequency spectra using the *realSFS* function with *-fold 1*. We  
29  
30 298 used *realSFS saf2theta* with *fold -1* to estimate per-site theta values and *thetaStat dostat* on folded SFS  
31  
32 299 and estimated theta values to estimate Tajima's D separately for each region. To estimate  $\pi$ , we divided  
33  
34 300 pairwise theta ( $tP$ ) by the number of sites compared (*nsites*) for each chromosome, and then averaged  
35  
36 301 this value over all chromosomes.

33 302 To estimate demographic history at different time scales, we used two demographic  
34  
35 303 reconstruction methods. First, we used a coalescent method based on the site frequency spectrum  
36  
37 304 (*stairwayplot2*, Liu and Fu 2015; Liu and Fu 2020) to infer demographic history over long time  
38  
39 305 periods. We then ran *stairwayplot2* using default recommended parameters for folded site frequency  
40  
41 306 spectra, with mutation rates of  $1.0 \times 10^{-8}$ , which has frequently been used as a default rate in studies of  
42  
43 307 fish species (Delrieu-Trottin *et al.*, 2020), and  $2.0 \times 10^{-9}$ , (Feng *et al.*, 2017), the measured mutation  
44  
45 308 rate in Atlantic Herring, and among the lowest recorded in a fish species, and time to maturity of 9.5  
46  
47 309 years, based on averaged Atlantic Halibut time to maturity (Nielsen 1986). To estimate recent changes  
48  
49 310 in demographic history, we also used the linkage-based method implemented in SNeP (Barbato *et al.*,  
50  
51 311 2015). This method infers recombination rates between markers based on physical position, and  
52  
53 312 linkage between markers at varying recombination distances is then used to estimate changes in  
54  
55 313 effective population size across time, with lower recombination rates between loci estimating older  
56  
57 314 demographic events. Because measures of  $N_e$  from SNeP are strongly sample size dependent, we use  
58  
59 315 this method to infer relative  $N_e$  across time only, by dividing each  $N_e$  estimate by maximum inferred  
60  
316  $N_e$ .

## Results

### Population structure and genetic differentiation

The strongest signals of genetic differentiation detected among individuals were associated with highly divergent regions on chromosome S15 and chromosome S18 (Figure 2A, Supplementary Figure 3A). These genomic regions correspond to a potential large structural variant (chromosome S15) and to a putative sex determining region on chromosome S18, based on clear separation of individuals on PC2 by phenotypically-assigned sex (Supplementary Figure 3, Supplementary Figure 4B, Einfeldt *et al.*, *in revision*). In PCA comparisons, the axis strongly associated with the divergent region on chromosome S15 explained 0.23% of genomic variation and was associated with clustering of individuals in three distinct groups, (Figure 2B, Supplementary Figure 4A), likely representing genotype combinations of two separate haplotypes. PC axis 2, primarily associated with sex differentiation, explained 0.22% of genomic variation (Supplementary Figure 3). We identified 986 outliers using *pcadapt*, 445 of which were found on chromosome S18, and 461 on chromosome S15, whereas 80 were on other chromosomes.

We also identified subtle genetic differentiation between the Gulf of St. Lawrence and Atlantic continental shelf (i.e., Scotia Shelf / Grand Banks regions). This differentiation was reflected in very low ( $F_{ST} = 0.0005$ , min SNP  $F_{ST} = 0$ , max SNP  $F_{ST} = 0.068$ ) but significant ( $p < 0.001$ ) divergence between regions, and clear separation of Gulf of St. Lawrence on PC axis 3 in the PCA analysis of the full dataset. The 861 SNPs in the top 1% of the  $F_{ST}$  distribution (mean  $F_{ST} = 0.018$ , max  $F_{ST} = 0.068$ ) were found across all 24 chromosomes (Figure 3A). Using *snmf* on the dataset with chromosomes S15 and S18 removed, cross entropy criterion suggested only  $K = 1$  ancestral groups, indicating very low overall genetic divergence between regions. PC and *snmf* analyses with  $F_{ST}$  outliers uncovered divergence between the Gulf of St. Lawrence individuals and those collected on the Atlantic continental shelf, as well as greatest cross entropy criterion support at  $K = 2$  (Figure 3B, 3C).

PCA and *snmf* on datasets with chromosomes S15 and S18 removed, and filtered for LD or with single SNPs per RAD locus retained revealed similar patterns of separation in PCA (Supplementary Figure 5), cross-entropy criteria at  $K=1$ , and similar values of significant  $F_{ST}$  for both datasets (0.0005,  $p < 0.001$ ). PCA within separate regions (Atlantic continental shelf, Gulf of St. Lawrence) did not reveal hierarchical spatial structure (Supplementary Figure 6 A,B), and  $F_{ST}$  comparisons between the most distant regions of the Atlantic continental shelf – Newfoundland and Grand Banks compared to the Gulf of Maine, did not reveal significant differentiation ( $F_{ST} < 0.0001$ ,  $p = 0.1$ ).

## Environmental association

Redundancy analysis also identified subtle genomic differentiation between the Gulf of St. Lawrence and the Atlantic continental shelf associated with environmental variation between these regions (Figure 2C). Environmental variables explained a small but significant proportion of overall genomic variation ( $p < 0.001$ , adjusted  $R^2 = 0.023\%$ ), with each environmental PC identified as significant in the model ( $p < 0.001$ ). The first environmental axis showed strongest association with the PC of dissolved oxygen variables, inferred from similar direction on RDA1 axis of the vector of oxygen PCs (Figure 2C). The observed pattern of environmental association was genome-wide with 261 loci exhibiting significant environmental associations, despite small combined variation explained (Figure 2D). We found that 49 (19%) of these loci were also  $F_{ST}$  outliers divergent between the Gulf of St. Lawrence and the Atlantic continental shelf (Figure 3A), whereas only 9 (3.5%) overlapped with autosomal *pcadapt* outliers outside of the putative structural variant on chromosome S15. In contrast, repeating this analysis with constraint by Latitude and Longitude revealed no significant associations between environmental variation and genome-wide divergence. However, we identified 260 significant outlier loci from the geography-constrained RDA, 44 of which were found in common between both sets of environmental outlier loci from both partial and full RDAs (9.2%), but only two loci of the 44 shared between RDA approaches matched  $F_{ST}$  outliers. RDA using only Latitude and Longitude revealed a significant association of Latitude with genomic variation ( $p < 0.001$ ), but also explained a small proportion of overall genomic variation (adjusted  $R^2 = 0.032\%$ ).

## Characterization of a putative structural variant

We identified individual variation on chromosome S15 that exhibited high divergence that did not correspond to geographic variation (Figure 4A, 4B), suggesting fine-scale genome architectural variation in Atlantic Halibut. Based on separation of individual scores on PC1 from PCA restricted to SNPs on chromosome S15 (Supplementary Figure 7), we assigned 349 individuals as homozygous for haplotype 1, 57 individuals homozygous for haplotype 2, and 328 heterozygous individuals. We found that these genotypes did not show significant deviation from HWE ( $p = 0.11$ ). We found a sharp rise in linkage disequilibrium ( $r^2 = 0.04$ , Figure 4C, 4D) and divergence between individuals homozygous for each haplotype ( $F_{ST} = 0.18$ ) in a large genomic region from approximately 5.75 to 12 Mbp (Figure 4B). These coordinates are rough estimates, as with a reference genome size of  $\sim 0.597$  Gbp, we have only mapped 33,076 RAD loci, corresponding to coverage of one RAD locus per  $\sim 18,000$  bp. LD and  $F_{ST}$  values were significantly ( $p < 10^{-10}$ , both tests) higher than the remainder of the chromosome ( $F_{ST} = 0$ , LD  $r^2 = 0.024$ ).  $F_{ST}$  and linkage between SNPs also showed correlated patterns in the divergent region

(Pearson's  $r^2 = 0.18$ ,  $p < 10^{-6}$ ), whereas no relationship between these statistics was found across the remainder of the chromosome (Fig 4D). We found elevated LD among all genotype groups at this region compared to the remainder of the chromosome (Supplementary Figure 8B,  $p < 0.001$  in all comparisons). Comparison of heterozygosity among individuals with different genotypes indicated a rise in heterozygosity among inferred heterozygotes in this region (Supplementary Figure 8B  $p < 0.001$ ), whereas homozygous individuals exhibited significantly reduced heterozygosity within this region relative to the remainder of the chromosome ( $p < 0.001$  in both comparisons). Using *inversion*, we found additional support for structural variation underlying this divergent region. This method indicated breakpoints for a putative inversion between 5.7 Mbp and 10.9 Mbp coinciding with the location of the divergent genomic region. Extracting gene information from the annotated genome revealed overlap with 232 annotated genes with gene symbols, but no significant overrepresentation of biological processes, (Supplementary File 1).

### Demographic history and genetic diversity

Estimates of genetic diversity were similar in both the Gulf of St. Lawrence and on the Atlantic continental shelf ( $H_e = 0.22$ ,  $H_o = 0.21$ ,  $\pi = 0.0021$ ) and the Gulf of St. Lawrence individuals ( $H_e = 0.22$ ,  $H_o = 0.21$ ,  $\pi = 0.024$ ). We did not find significant differences between regions in either estimate of diversity. Estimates of LD-based  $N_e$  were also infinite in both regions. We identified small, negative Tajima's D estimates in both the Gulf of St. Lawrence (-0.07) and Atlantic continental shelf (-0.23).

Reconstructions of demographic history using using *stairwayplot2* suggest that expansion of Atlantic Halibut population sizes coincided with warming during the end of Last Glacial Period (~11,000 years ago). Using both upper ( $1.0 \times 10^{-8}$ ) and lower bound mutation rates ( $2.0 \times 10^{-9}$ ), we found a period of increasing  $N_e$  was observed between the Mid-Holocene Warm Period (~5000-7000 years ago) and the end of the Last Glacial Maximum (~19,000 years ago, Figure 5A,B). These reconstructions exhibit large confidence intervals and plateaus of inferred  $N_e$  over the recent past: ~2000 years for the upper bound mutation rate and ~5,000 years for the lower bound mutation rate. Estimates of demographic change from *SNeP* identified ongoing decline during the past ~7000 years (Figure 5C).

### Discussion

In this study, we conduct the first large-scale investigation of genomic diversity in Atlantic Halibut using high-density genomic markers and uncover previously unrecognized genetic structure in

1  
2 416 this species. We identify subtle genomic differentiation associated with divergence between the Gulf of  
3  
4 417 St. Lawrence and the Atlantic continental shelf, overlapping with loci significantly associated with  
5  
6 418 environmental gradients. In contrast to subtle oceanographic structuring, we find that the majority of  
7  
8 419 genetic variation is attributable to a large divergent region consistent with a putative chromosomal  
9  
10 420 inversion, variable among individuals across the Northwest Atlantic. Estimation of demographic  
11  
12 421 histories revealed contrasting patterns of high  $N_e$  coinciding with the end of the Last Glacial Period,  
13  
14 422 and declines over more recent time-frames. Together, these results indicate that Atlantic Halibut  
15  
16 423 exhibits both genome-wide, environment-associated population structure and fine-scale individual  
17  
18 424 variation associated with a divergent chromosomal region indicating multiple sources of genomic  
19  
20 425 differentiation in this species.

19 426 Our analyses of population structure identified a subtle but significant pattern of population  
20  
21 427 divergence between the Atlantic continental shelf and the Gulf of St. Lawrence. The small proportion  
22  
23 428 of genetic variation explained, and low but significant  $F_{ST}$  observed here, are both consistent with weak  
24  
25 429 structuring identified in other high gene flow marine species (Pespeni and Palumbi 2013; Babin *et al.*,  
26  
27 430 2017; Jiménez-Mena *et al.*, 2020). These findings contrast with a lack of divergence observed in a  
28  
29 431 microsatellite study of the Northwest Atlantic (Reid *et al.*, 2005), highlighting the capacity of large  
30  
31 432 panels of genomic markers to detect subtle population structure (Bradbury *et al.*, 2010; Gagnaire *et al.*,  
32  
33 433 2015; Benestan *et al.*, 2015). This observation is consistent with the hypothesis that in marine species  
34  
35 434 with large effective population size, long timeframes may be required for appreciable genome-wide  
36  
37 435 differentiation to accumulate by drift, reflected in significant  $F_{ST}$  values, even in instances of low or  
38  
39 436 zero connectivity (Hauser and Carvalho 2008). Under these conditions, even low levels of dispersal  
40  
41 437 will add to time required for differentiation, making identification of significant divergence in marine  
42  
43 438 species challenging (Gagnaire *et al.*, 2015). We uncover significant differentiation between regions,  
44  
45 439 despite high effective population size and limited time for contemporary populations structure to  
46  
47 440 develop following deglaciation of the Northwest Atlantic (Reid *et al.*, 2005). This observation suggests  
48  
49 441 forces beyond drift have driven contemporary population structure in the Northwest Atlantic, and we  
50  
51 442 find environmental variation significantly explains a small proportion of genomic variation in this  
52  
53 443 species. Individual scores on RDA axes similarly revealed separation between Gulf of St. Lawrence  
54  
55 444 and Atlantic continental shelf individuals, indicating oceanographic features may contribute to genetic  
56  
57 445 divergence between these regions. This pattern was not significant after constraining RDA by  
58  
59 446 geographic variation, indicating disentangling patterns of geographic separation and environmental  
60  
447 variation may be difficult in this system. However, comparisons of differentiation between distant sites  
448 along the Atlantic continental shelf did not reveal significant differentiation, indicating some feature

1  
2 449 specific to the Gulf of St. Lawrence has led to subtle but detectable divergence. These findings are  
3  
4 450 concordant with the recent identification of relatively high site fidelity of Atlantic Halibut in tagging  
5  
6 451 studies (den Heyer *et al.*, 2012; Le Bris *et al.*, 2018) as well as low connectivity and independence of  
7  
8 452 population dynamics in this species (Boudreau *et al.*, 2017).

9 453 Using a test of multi-locus environmental association, we uncovered a genome-wide basis of  
10  
11 454 environmental association with many loci dispersed throughout the genome exhibiting association with  
12  
13 455 temperature, oxygen, and salinity gradients. Environmental variation has been found to coincide with  
14  
15 456 barriers to genetic exchange of locally adapted loci across marine species, leading to genomic  
16  
17 457 divergence and population structure (Van Wynngarden *et al.*, 2017; Stanley *et al.*, 2018; Kess *et al.*,  
18  
19 458 2020). The identification of genome-wide environmental association in Atlantic Halibut matches recent  
20  
21 459 findings of similar genomic signatures of adaptation to environmental gradients in other marine species  
22  
23 460 (Bay and Palumbi 2014; Healy *et al.*, 2018; Rey *et al.*, 2020). Multiple environmental gradients have  
24  
25 461 been found to dictate divergence and population structure, including temperature (Xuereb *et al.*, 2019,  
26  
27 462 Benestan *et al.*, 2016), salinity (Healy *et al.*, 2018), and oxygen (Berg *et al.*, 2015). Here, we find that  
28  
29 463 differences in available dissolved oxygen between the Gulf of St. Lawrence and the Atlantic  
30  
31 464 continental shelf are associated with subtle genomic divergence, contrasting recent identification of  
32  
33 465 winter bottom temperature driving multi-species clinal differentiation in the Northwest Atlantic  
34  
35 466 (Stanley *et al.*, 2018). Recent identification of similar genetic structure in Greenland Halibut (Carrier *et*  
36  
37 467 *al.*, 2020), as well as low oxygen availability in the Gulf of St. Lawrence (Brennan *et al.*, 2016) suggest  
38  
39 468 adaptation to hypoxia as a potential mechanism driving environmental associations observed in this  
40  
41 469 study. We also uncovered overlap between loci significantly associated with divergence between the  
42  
43 470 Gulf of St. Lawrence and the Atlantic continental shelf, indicating reduced gene flow between these  
44  
45 471 regions may correspond to different environmental tolerances. Despite identifying many significantly  
46  
47 472 associated loci, their association with environmental gradients was weak and differentiation was  
48  
49 473 relatively low even at outlier loci, suggesting that environmental adaptation has manifested in small  
50  
51 474 allele frequency shifts (Le Corre and Kremer 2012; Flaxman *et al.*, 2014), compared to other high  
52  
53 475 dispersal marine species which exhibit large regions of genomic divergence (Lamichhaney *et al.* 2017;  
54  
55 476 Kess *et al.* 2020). However, some caution is warranted in interpreting the role of environmental outliers  
56  
57 477 identified here, as habitat and spawning-site fidelity have been identified across the Northwest Atlantic,  
58  
59 478 and thus environmental outlier loci identified here may also represent loci differentiated between  
60  
61 479 regions due to divergence covarying with the differing environments between these localities (Gatti *et*  
62  
63 480 *al.*, 2020; Le Bris *et al.*, 2018).

1  
2 481 We identified a region of large genomic divergence on chromosome S15 that explained the  
3  
4 482 majority of genetic variation, and exhibited high linkage and  $F_{ST}$ , consistent with a chromosomal  
5  
6 483 rearrangement. We find that this region meets several criteria consistent with indirect evidence of a  
7  
8 484 chromosomal inversion: elevated divergence and LD in the total dataset, and reduced heterozygosity  
9  
10 485 among homozygous individuals relative to heterozygous individuals (Merot *et al.*, 2020). This region  
11  
12 486 was responsible for the primary axis of genetic variation among individuals; the correlated divergence  
13  
14 487 among linked SNPs (Lotterhos 2019), suggests divergence of this locus as a single “supergene”  
15  
16 488 (Thompson and Jiggins 2014). With widespread availability of high-quality genomes and genotype  
17  
18 489 data, chromosomal rearrangements are increasingly being identified as important genomic architectural  
19  
20 490 features underlying supergenes and associated with adaptive phenotypes in marine species, including  
21  
22 491 migratory and spawning differences in Atlantic Cod (Kess *et al.*, 2019), Atlantic Herring (Lamichhaney  
23  
24 492 *et al.*, 2017), and Rainbow Trout (Pearse *et al.*, 2019). Recent exploratory studies in migratory and high  
25  
26 493 gene flow species have also identified evidence consistent with rearrangements, without obvious  
27  
28 494 phenotypic or environmental links, as observed here (Cayuela *et al.*, 2020; Longo *et al.*, 2020).  
29  
30 495 Rearrangements and inversions may be especially important in species with high dispersal capability,  
31  
32 496 enabling trait divergence despite ongoing gene flow (Hooper and Price 2017), and consistent with fine-  
33  
34 497 scale variation despite gene flow we find within-region variation in rearrangement genotypes. Future  
35  
36 498 genome-wide association studies with behavioural and phenotypic variation in Atlantic Halibut may aid  
37  
38 499 in clarifying the role of this putative rearrangement. Additionally, we present only indirect evidence for  
39  
40 500 structural variation; this uncertainty may be resolved by future long-read sequencing which can directly  
41  
42 501 characterize rearrangements.

38 502 We uncovered similar patterns of genetic diversity and large effective population size across  
39  
40 503 both geographic regions, and predictions of similar demographic histories. Large contemporary  
41  
42 504 effective population sizes, inferred from infinite LD-based  $N_e$  estimates, may partially be attributable to  
43  
44 505 recent population expansions occurring in Canadian waters, but consistent large effective population  
45  
46 506 sizes were inferred despite qualitative patterns of decline in our LD based reconstruction of  
47  
48 507 demographic history, consistent with the potential for high fecundity in this species (Trzcinski and  
49  
50 508 Bowen 2016). Demographic reconstructions in *stairwayplot2* revealed population expansion occurring  
51  
52 509 between ~5000 and 19,000 years, depending on specified mutation rate, coinciding with either the end  
53  
54 510 of the Mid-Holocene Warm Period (~5000-7000 years ago) or following the Last Glacial Maximum  
55  
56 511 (LGM). Demographic changes coinciding with climatic variation may be due to changes in abundance  
57  
58 512 of prey or competitors, or changes in availability of suitable habitat (Hoegh-Guldberg and Bruno 2010;  
59  
60 513 Cristofari *et al.*, 2018; Vijay *et al.*, 2018). The expansion of  $N_e$  associated with transition to the



1  
2 514 Holocene suggests that either changes in ocean temperature or deglaciation of suitable habitat in the  
3  
4 515 Northwest Atlantic may have enabled population expansion.

5 516         Some caution is warranted in over-interpreting these results, as fluctuations in migration and  
6  
7 517 population structure may also generate patterns of demographic change (Mazet *et al.*, 2016).  
8  
9 518 Additionally, some uncertainty is expected in our results, as genome-level mutation and recombination  
10  
11 519 rate estimates for Atlantic Halibut are not available. We compensate for these limitations by estimating  
12  
13 520 recent demographic changes using linkage-disequilibrium, instead identifying evidence of potential  
14  
15 521 declines during the last ~7000 years, coinciding with the beginning of the Mid-Holocene Warm Period.  
16  
17 522 The discrepancy in observations from these two methods may reveal their sensitivity to demographic  
18  
19 523 changes occurring at more recent or distant timeframes. *SNeP* is limited in utility to infer older  
20  
21 524 demographic changes without very high-density SNP panels (Barbato *et al.*, 2015), and similar LD  
22  
23 525 based methods can be downwardly biased towards detection of ongoing decline due to recent  
24  
25 526 population declines (Hollenbeck *et al.*, 2016), as those that have been documented in Atlantic Halibut  
26  
27 527 reflecting recent extirpations due to over-fishing (Shackell *et al.* 2012; Trzcinski and Bowen 2016).  
28  
29 528 Similarly, the large confidence intervals and plateaus in  $N_e$  over the last ~2,000-5,000 years from  
30  
31 529 *stairwayplot2*, dependent on specified mutation rate, suggest low resolution of recent demographic  
32  
33 530 history. Although the exact cause of historical changes in diversity cannot be inferred, their coincidence  
34  
35 531 with changes in climate supports the hypothesis that the demographic history of Atlantic Halibut may  
36  
37 532 have been impacted by past climatic fluctuations.

38  
39 533         Our results here provide insight into the magnitude and geographic scale of genomic  
40  
41 534 differentiation in marine species, and are directly applicable to the conservation and management of  
42  
43 535 Atlantic Halibut in the Northwest Atlantic. Our observation of environment-associated genomic  
44  
45 536 differentiation between the Atlantic continental shelf and the Gulf of St. Lawrence provides further  
46  
47 537 support for independent management of these regions (e.g., DFO 2015a, 2015b). Our observations  
48  
49 538 indicate subtle genetic differentiation between stocks matching known differences in behaviour and life  
50  
51 539 history (den Heyer *et al.*, 2012; Le Bris *et al.* 2018), suggesting some limits to genetic exchange  
52  
53 540 between regions. The observed genome-wide environmental associations are consistent with adaptation  
54  
55 541 to different environmental conditions (e.g. oxygen availability), and may further reduce gene flow  
56  
57 542 between regions. Additionally, further examination of the link between ecologically-distinct  
58  
59 543 phenotypes and the newly identify putative structural variant is suggested and may inform the  
60  
61 544 conservation of key phenotypic diversity, as has recently been considered in other marine species  
62  
63 545 (Waples 2018).  
64  
65 546

1  
2  
3  
4  
5  
6  
7  
8  
9  
10  
11  
12  
13  
14  
15  
16  
17  
18  
19  
20  
21  
22  
23  
24  
25  
26  
27  
28  
29  
30  
31  
32  
33  
34  
35  
36  
37  
38  
39  
40  
41  
42  
43  
44  
45  
46  
47  
48  
49  
50  
51  
52  
53  
54  
55  
56  
57  
58  
59  
60

**Conclusion**

Our study provides the first evidence of genome-wide population structure in Atlantic Halibut, revealing genomic divergence between the Gulf of St. Lawrence and Atlantic continental shelf regions. We also identify a large putative structural variant displaying high differentiation and linkage disequilibrium, indicating the presence of a potential supergene. Estimates of demographic history indicate potential ongoing declines in this species, and a more distant population expansion coinciding with the end of the Last Glacial Period. Together, these results reveal multiple previously uncharacterized sources of genomic differentiation in Atlantic Halibut.

For Review Only

## 557 **Acknowledgements**

558 For facilitating sampling of Atlantic Halibut, we thank: Bruce Chapman of the Atlantic Halibut  
559 Council, Geryy and Gary Dedrick of the Shelburne County Quota Group, Lori Baker from the Eastern  
560 Shore Fisherman's Protective Association, Erin Caruthers and Miranda McGrath from FFAW., Alber  
561 Moore and Dylann Buchannan and Fisheries Observers from Javitech Atlantic, and Derrick Lambert  
562 and Fisheries Observers from Seawatch Inc. We thank Michael Kersula and the Maine Department of  
563 Marine Resources, and Esther Román-Marcotte and Jose Luis Del Rio from the Spanish Institute of  
564 Oceanography for providing Atlantic Halibut tissue samples. We thank Christopher McGuire and  
565 Jocelyn Runnebaum of The Nature Conservancy, Richard McBride from the National Oceanic and  
566 Atmospheric Administration, George Maynard of the Cape Cod Commercial Fishermen's Alliance, and  
567 Scott Elzey from the Massachusetts Division of Marine Fisheries for additional coordination collection  
568 of Atlantic Halibut Samples. We thank Lorraine Hamilton for organizing RAD library preparation, and  
569 the McGill University and Génome Québec Innovation Centre for genotyping RAD libraries.  
570 Sequencing of the reference genome sequence was conducted by the Vertebrate Genome Project.  
571 Funding and support for this project was through the Ocean Frontier Institute and the Department of  
572 Fisheries and Oceans Canada Genomics Research and Development Initiative, as well as an NSERC  
573 Visiting Postdoctoral Fellowship.

## 575 **Author Contributions**

576 T.K., I.R.B., D.R., and P.B. designed the study. T.K and T.E. conducted data analysis. T.K. wrote the  
577 manuscript and all authors contributed to editing and revising the manuscript.

## 579 **Data Availability**

580 Raw reads will be uploaded to the NCBI short read archive on publication. Files with genotypic  
581 information for all individuals and a metadata file of individual location and environmental parameters  
582 will be uploaded to dryad on publication. All scripts used in this study are available at:

583 [https://github.com/TonyKess/Halibut\\_RADseq](https://github.com/TonyKess/Halibut_RADseq)

**Table 1. Sampled regions, sampling trips, number of samples per trip, time of sampling, and gear used to collect 768 Atlantic Halibut tissue samples used for RAD sequencing library preparation.**

Region Sampled	Sampling trip	Number of samples	Sampling time	Sampling gear information
Gulf of St. Lawrence	DFO 2017 Gulf Longline Survey	76	Fall 2017	Hooked line
Gulf of St. Lawrence	DFO Teleost-14 Trawl Survey	83	August 2017	Trawl
Gulf of Maine/Georges Bank (NAFO 5Y and 5Ze)	The Nature Conservancy-Cape Cod Industry samples	42	Summer – Winter 2017	Gillnet
Gulf of Maine	Maine Department of Marine Resources – Gulf of Maine Survey	17	2018	Trawl
Newfoundland & Grand Banks	DFO Newfoundland Multi-species sSampling	17	Spring – Fall 2017	Hooked line
Newfoundland & Grand Banks	DFO 3Ps Halibut Port Sampling	45	November 2017	Line – hook sizes 15 – 16
Newfoundland & Grand Banks	Spanish Institute of Oceanography 3NO Survey	16	June 2018	-
Flemish Cap	Spanish Institute of Oceanography Flemish Cap Survey	11	Summer 2018	-

Newfoundland & Grand Banks, Scotian Shelf, Gulf of St. Lawrence (Cabot Strait)	DFO 2018 Longline Survey	461	Spring – Summer 2018	Hooked line
--	-----------------------------	-----	-------------------------	-------------

588

For Review Only

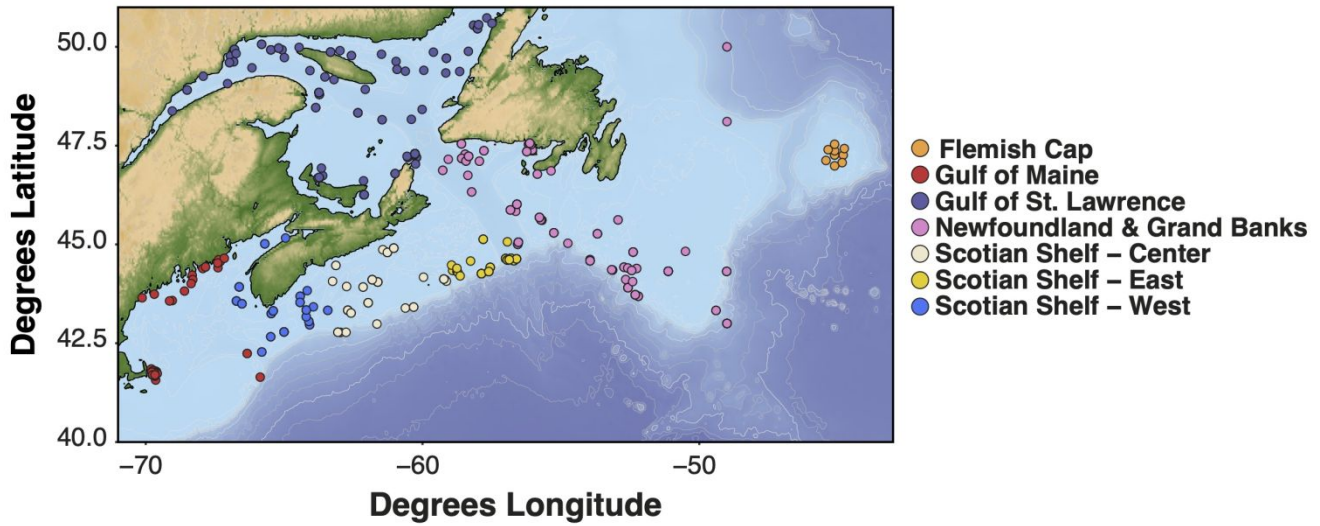
1  
2 589  
3  
4 590  
5 591  
6  
7 592  
8

Table 2. Number of SNPs, RAD loci, and strand mapping rates for SNP panels with different levels of filtering applied.

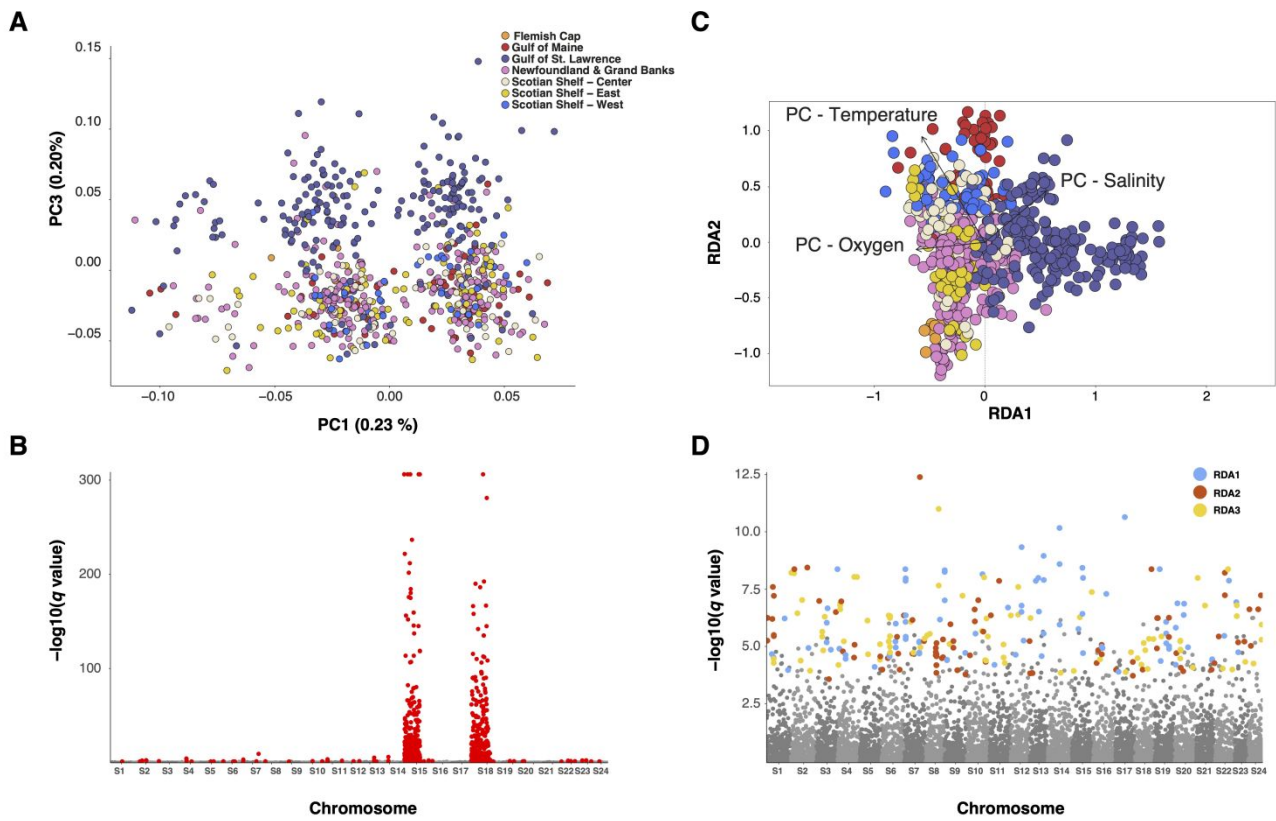
<b>SNP panel and filtering step</b>	<b>SNPs</b>	<b>RAD loci</b>	<b>Proportion SNPs mapped to positive strand</b>
Stacks exported	175,318	43,840	0.499
Filtered for minimum 90% genotyping per SNP, minimum read depth 15	89,801	33,988	0.497
Filtered for HWE	86,043	33,076	0.498
Filtered for sex locus and putative inversion	62,213	29,592	0.498
Filtered for LD, sex locus and putative inversion	61,662	29,550	0.498
Filtered to single SNP per RAD locus, sex locus and putative inversion	29,913	29,913	0.498

9  
10  
11  
12  
13  
14  
15  
16  
17  
18  
19  
20  
21  
22  
23  
24  
25  
26  
27  
28  
29  
30  
31  
32  
33  
34  
35  
36 593  
37  
38  
39  
40  
41  
42  
43  
44  
45  
46  
47  
48  
49  
50  
51  
52  
53  
54  
55  
56  
57  
58  
59  
60

1  
2 594 **Figure 1. Sampling locations of 734 Atlantic Halibut samples genotyped with RAD loci, coloured**  
3 595 **by sampling region.**  
4 596



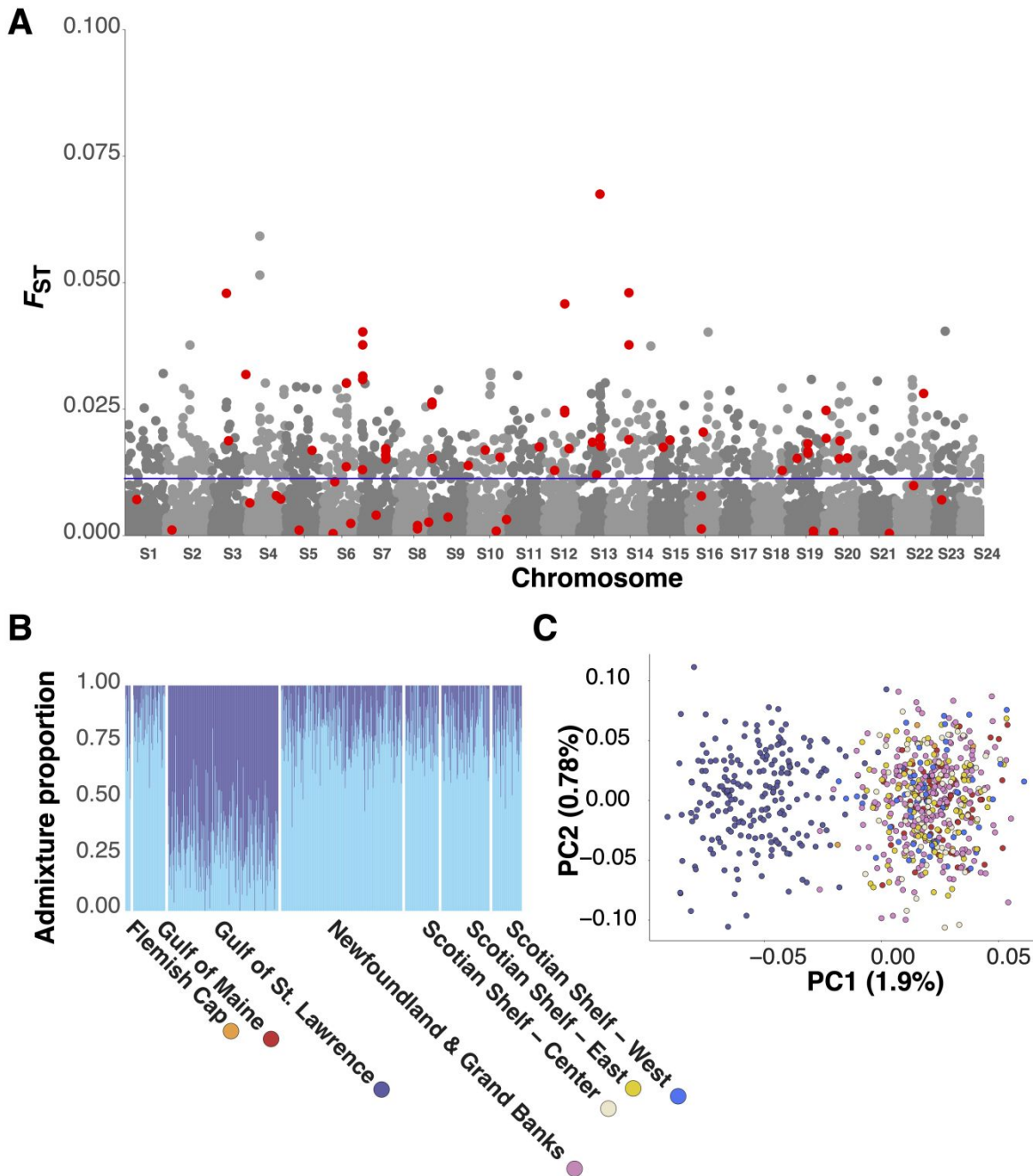
**Figure 2. Principal component analysis (PCA) scores of 734 individuals on PC1 and PC3 axes from PCA on 86,043 SNPs, highlighting population structure (PC3) and a putative inversion (PC1) (A), q values of SNP association with K =3 retained PC axes, with outliers ( $q < 0.05$ ) highlighted in red (thinned post-analysis to 15,000 randomly-thinned SNPs for visualization), (B), redundancy analysis of 734 individuals with principal components of temperature, dissolved oxygen and salinity (C), q values of SNP association with K =3 retained RDA axes, with outliers for each axis ( $q < 0.05$ , canonical score  $> 99.9^{\text{th}}$  percentile) highlighted (thinned post-analysis to 15,000 randomly-thinned SNPs for visualization), (D)**



610  
611

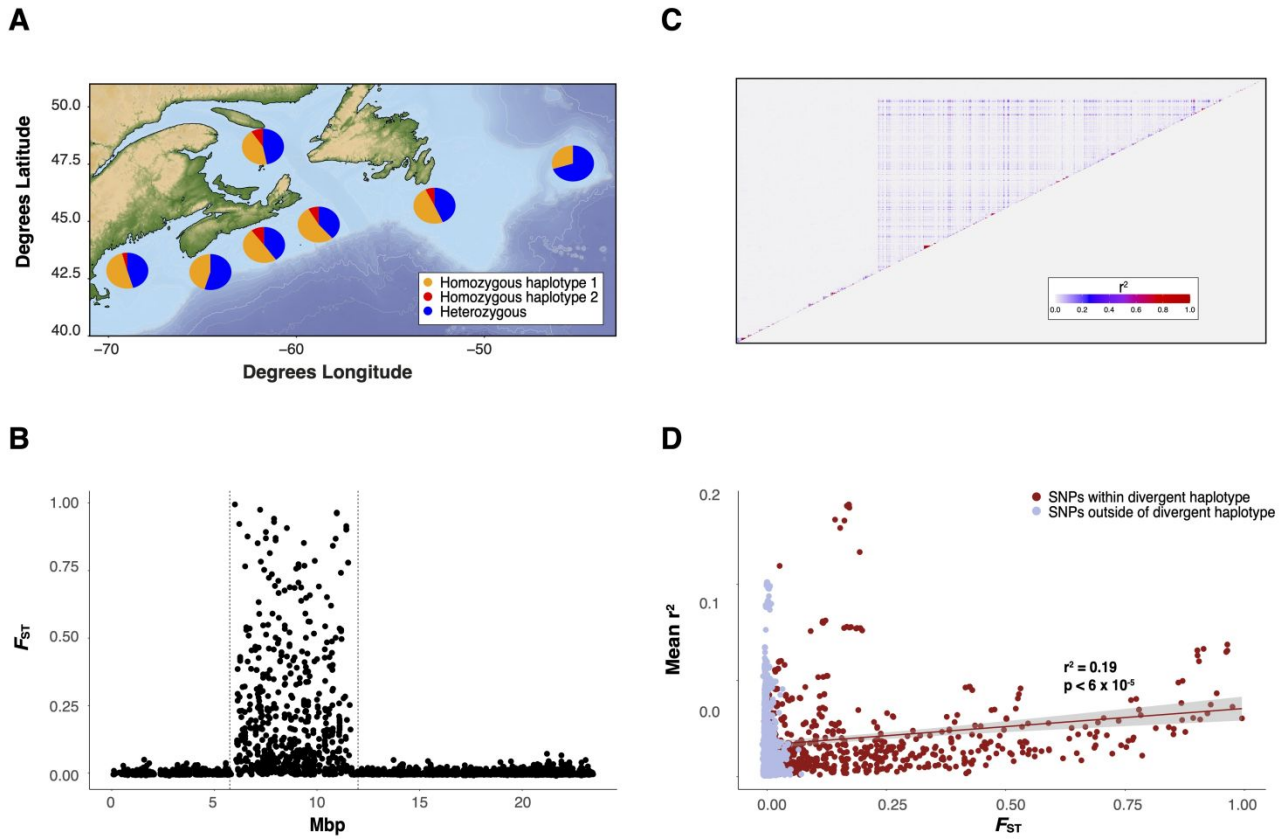


Figure 3. Distribution of  $F_{ST}$  between Gulf of St. Lawrence and Scotian Shelf and Grand Banks region (thinned post-analysis to 15,000 randomly-thinned SNPs for visualization), significant outliers with  $F_{ST} > 99^{\text{th}}$  percentile above the significance line, and RDA outliers highlighted in red (A), admixture proportions from sparse non-negative matrix factorization (B) and PCA scores (C) of 734 individuals using 861 outlier SNPs.



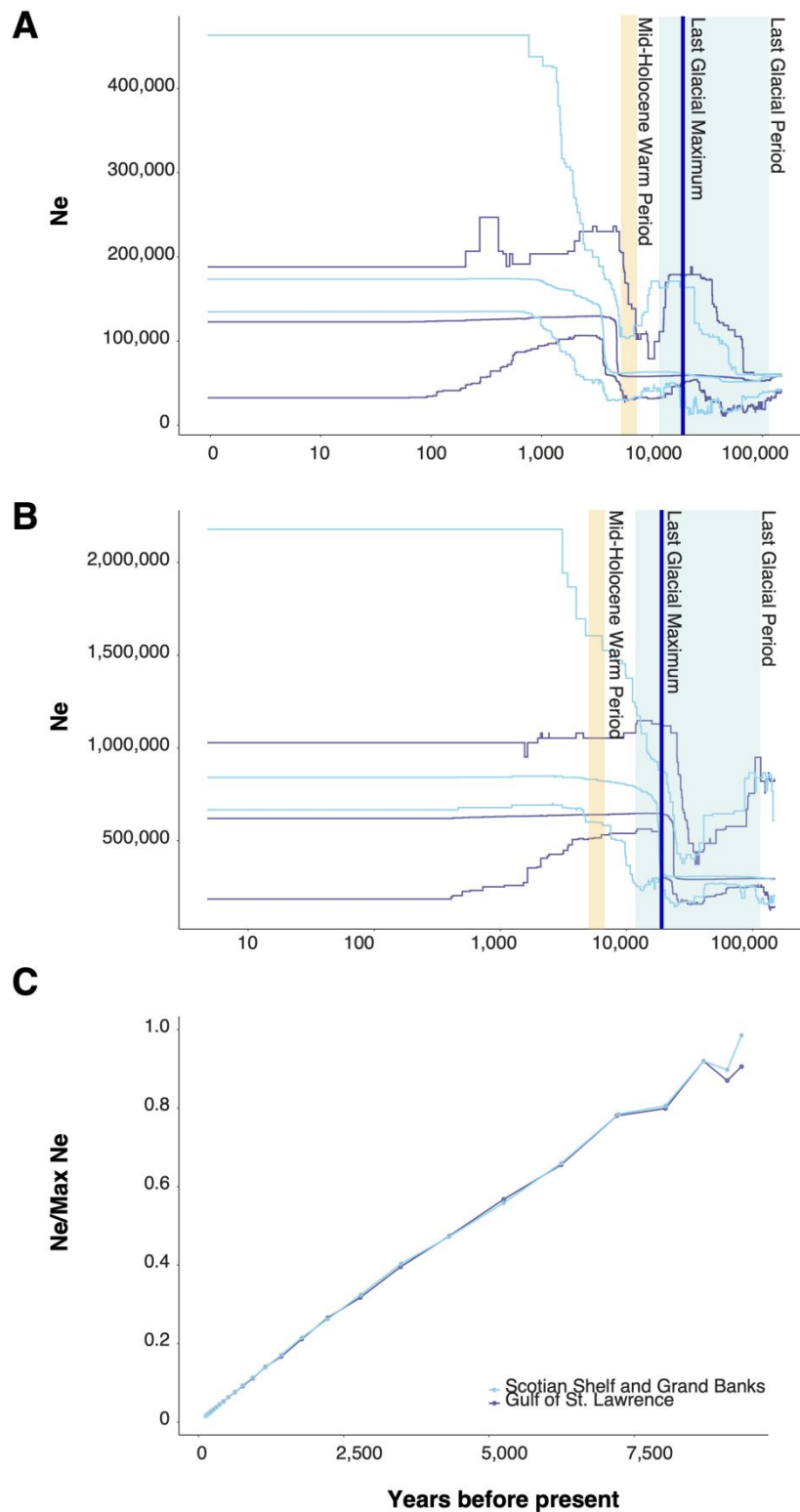
619

**Figure 4. Percentage of each genotype of the chromosome 15 putative structural variant in each sampling region (A),  $F_{ST}$  between individuals homozygous for haplotype 1 and haplotype 2 across chromosome 15 (B), a heatmap of LD from 4 Mbp to 13 Mbp on chromosome S15 (C), and Pearson's  $r^2$  correlation between LD ( $r^2$ ) of each SNP with 50 adjacent SNPs and  $F_{ST}$  across chromosome 15, compared within the putative structural variant region (red) and outside of it (blue) (D).**

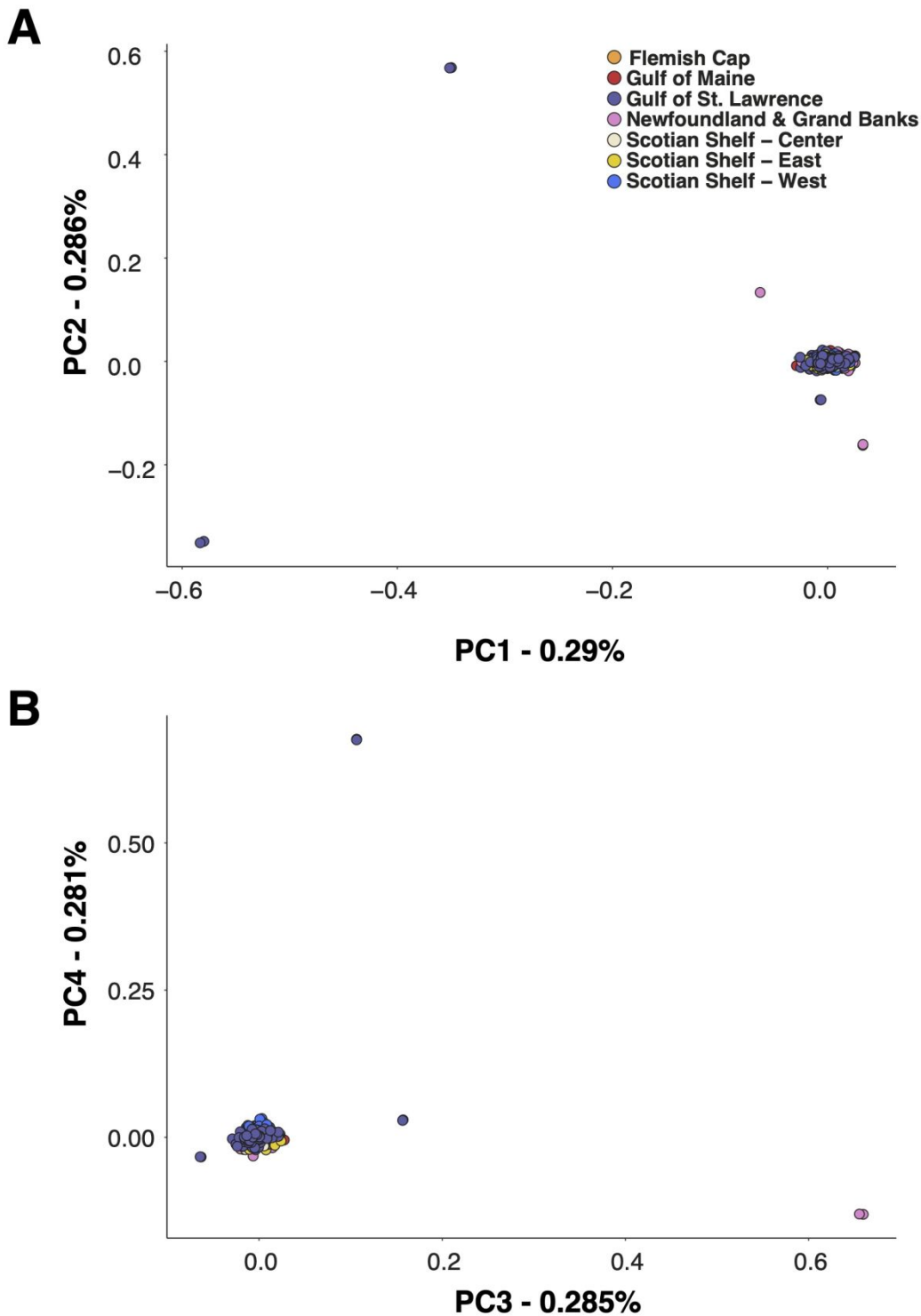


627

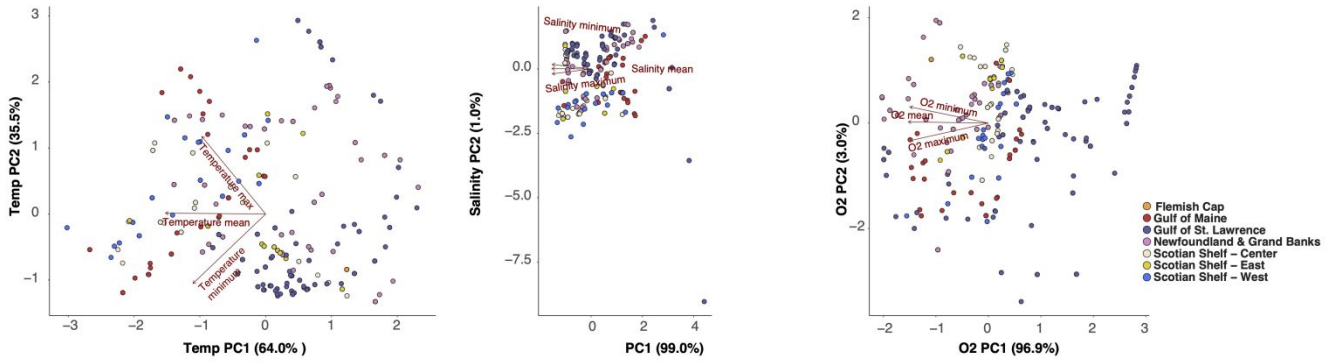
1  
2 628 **Figure 5. Reconstruction of effective population size ( $N_e$ ) over time for Gulf of St. Lawrence and**  
3 629 **Atlantic continental shelf regions using *stairwayplot2* with mutation rate  $1.0 \times 10^{-8}$  (A) and**  
4 630 **mutation rate  $2.0 \times 10^{-9}$ , (B), and *SNeP* (C).**  
5 631  
6 632  
7 633  
8 634  
9 635



Supplementary Figure 1. Individuals demonstrating potential long-distance movement inferred from principal component analysis on all SNP loci (PCA), identified by scores on PC1, PC2 (A), PC3, and PC4.



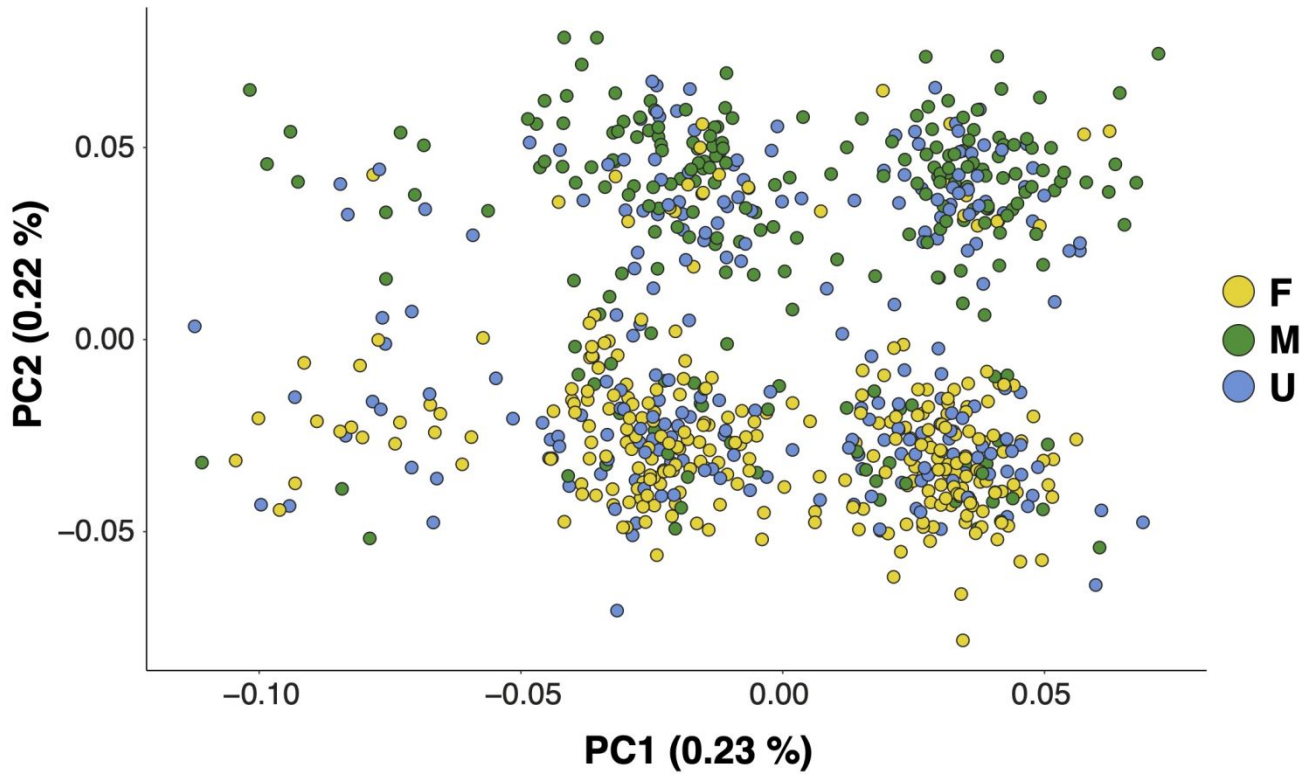
640 **Supplementary Figure 2. PCA biplots for PCs of combined temperature, salinity, and oxygen**  
641 **environmental variables.**



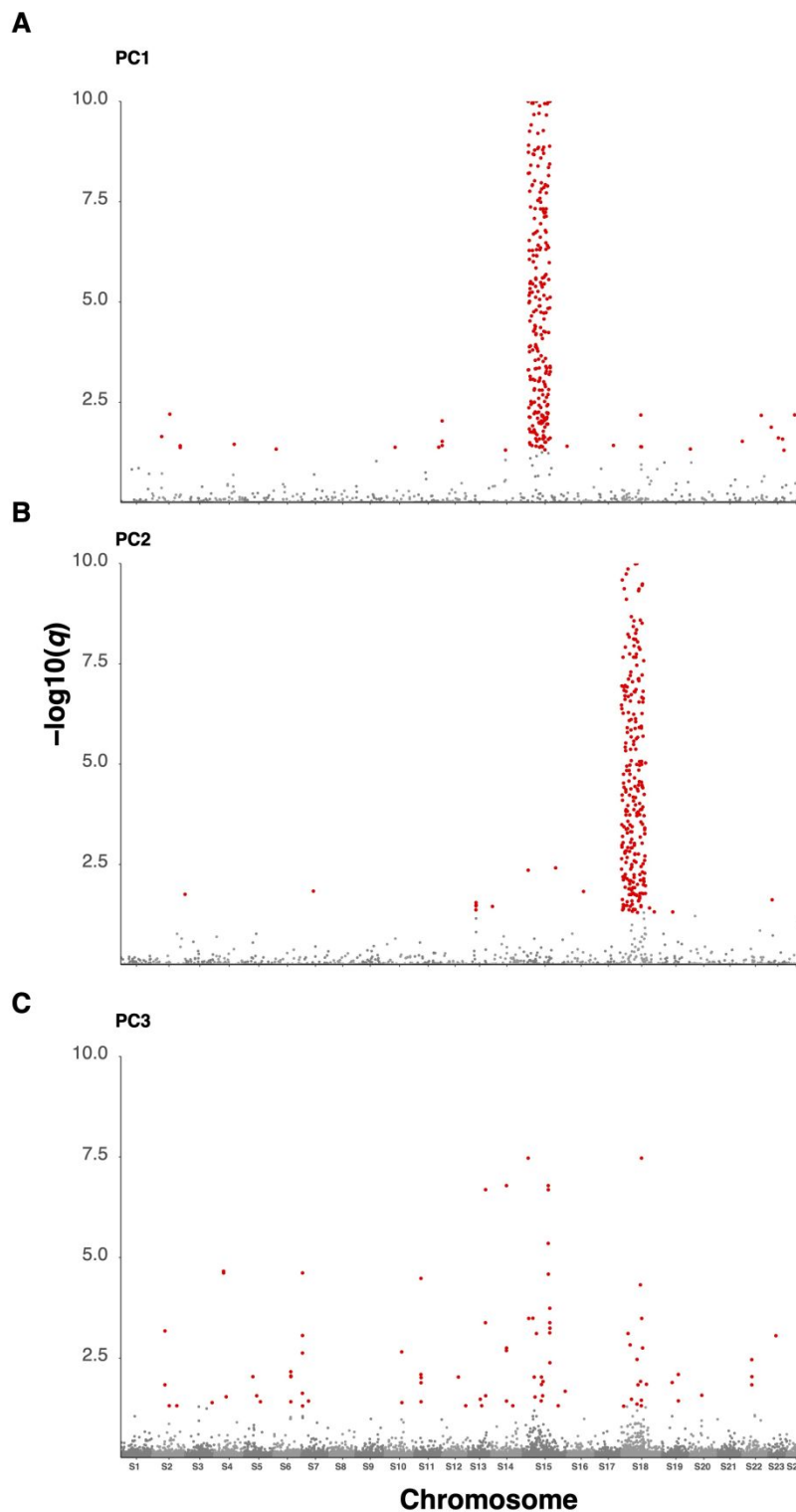
643

For Review Only

1  
2 644 **Supplementary Figure 3. Identification of a sex-associated region on chromosome 18 based on**  
3 645 **principal component analysis (PCA) scores of 734 individuals on PC2 from PCA on 86,043 SNPs**  
4 646  
5 647  
6 648  
7

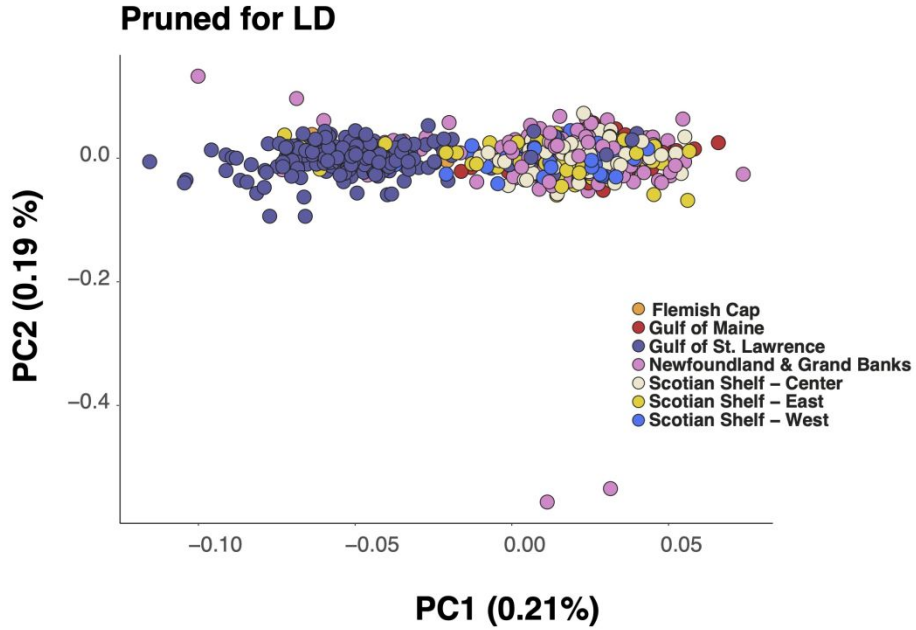


1  
2 649 **Supplementary Figure 4.  $-\log_{10}(q)$  values of SNP association with PC1, A) PC2, B) and PC3 C),**  
3 650 **with outliers ( $q < 0.05$ ) highlighted in red (thinned post-analysis to 15,000 randomly-thinned**  
4 651 **SNPs for visualization).**  
5 652  
6 653

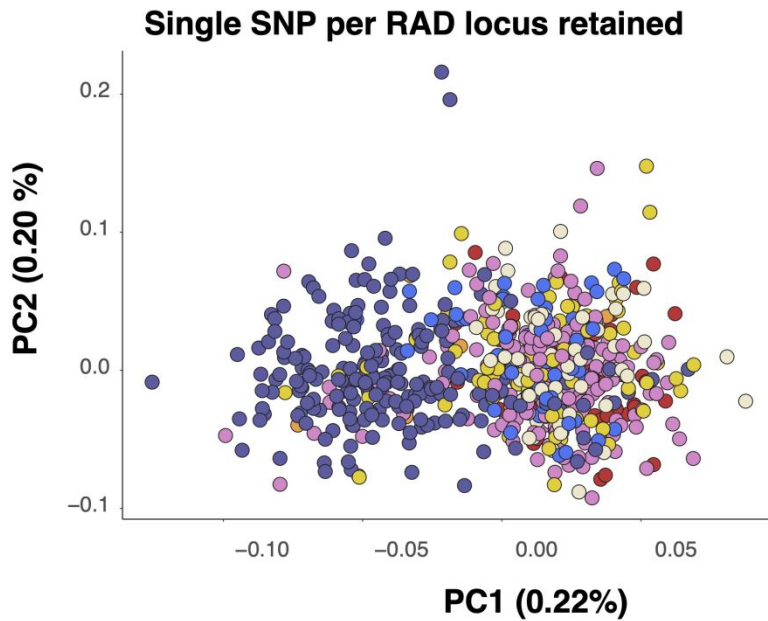


1  
2 654  
3 655 **Supplementary Figure 5. Principal component analysis (PCA) scores of 734 individuals on PC1**  
4 656 **and PC2 axes from PCA on 61,662 SNPs filtered for LD and with chromosomes S15 and S18**  
5 657 **removed (A), and 29,913 SNPs filtered to retain a single SNP per RAD locus, and with**  
6 658 **chromosomes S15 and S18 removed.**  
7  
8 659

9 **A**

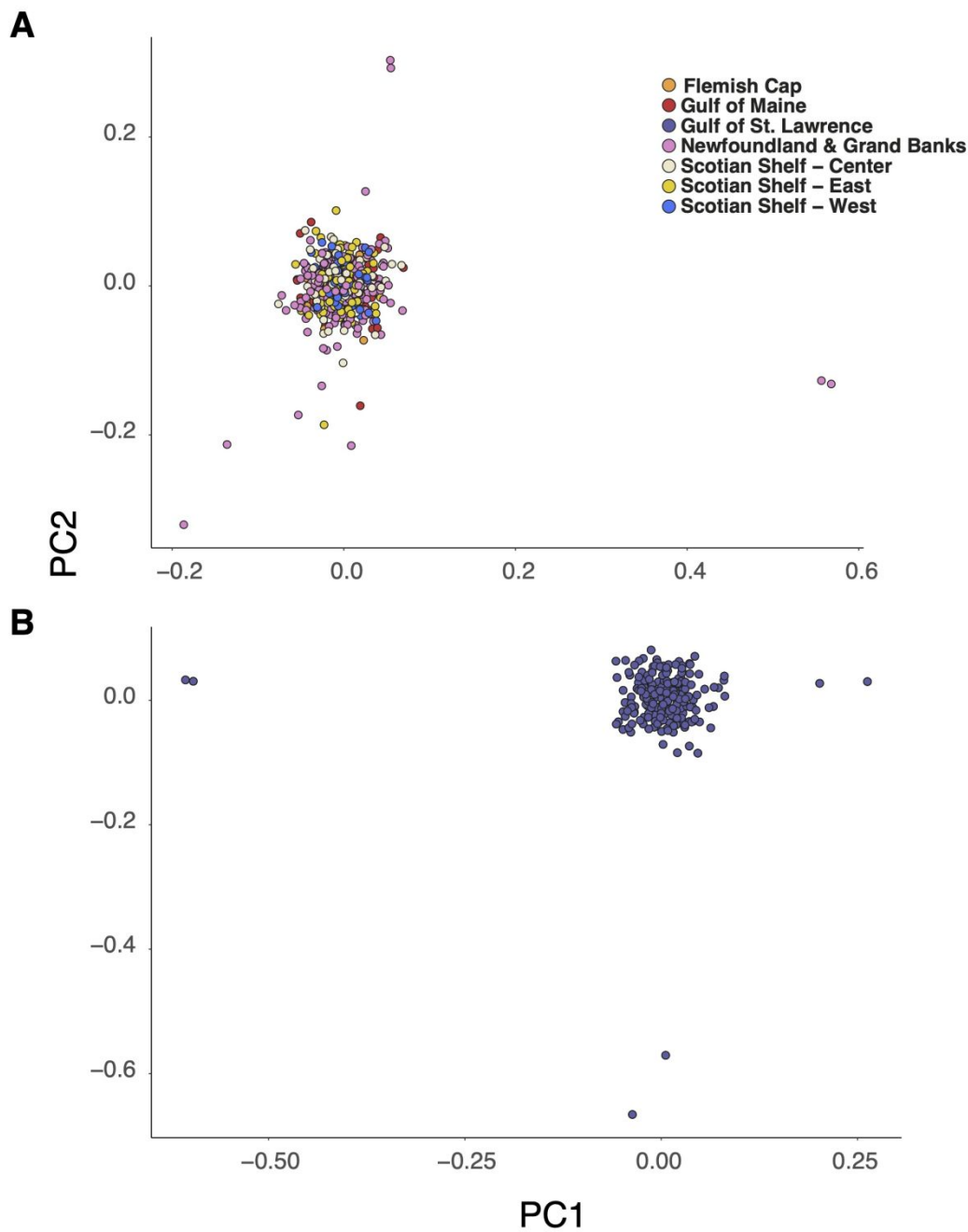


30 **B**

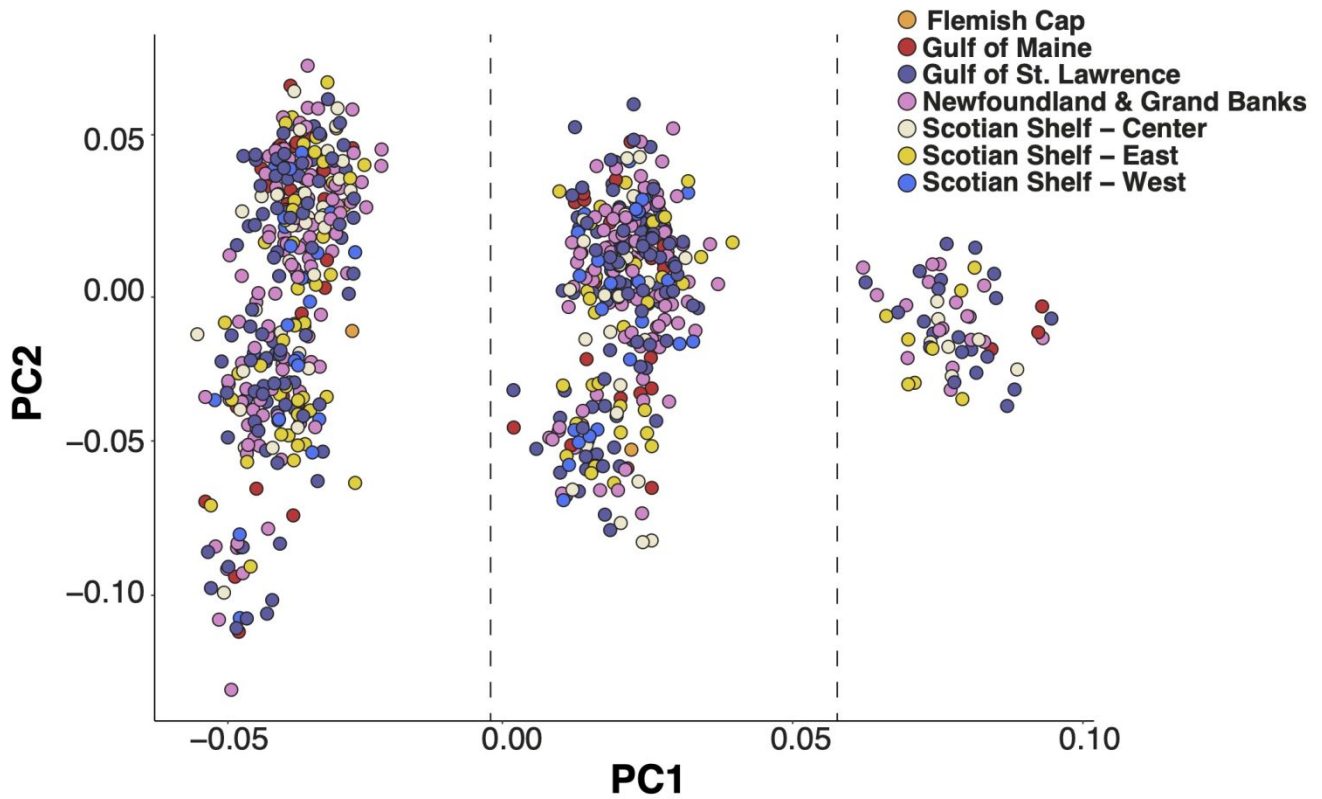




Supplementary Figure 6. Principal component analysis (PCA) scores on PC1 and PC2 axes from PCA on 62,213 SNPs with chromosomes S15 and S18 removed on 523 individuals from the Atlantic continental shelf (A), and 211 individuals from the Gulf of St. Lawrence (B).

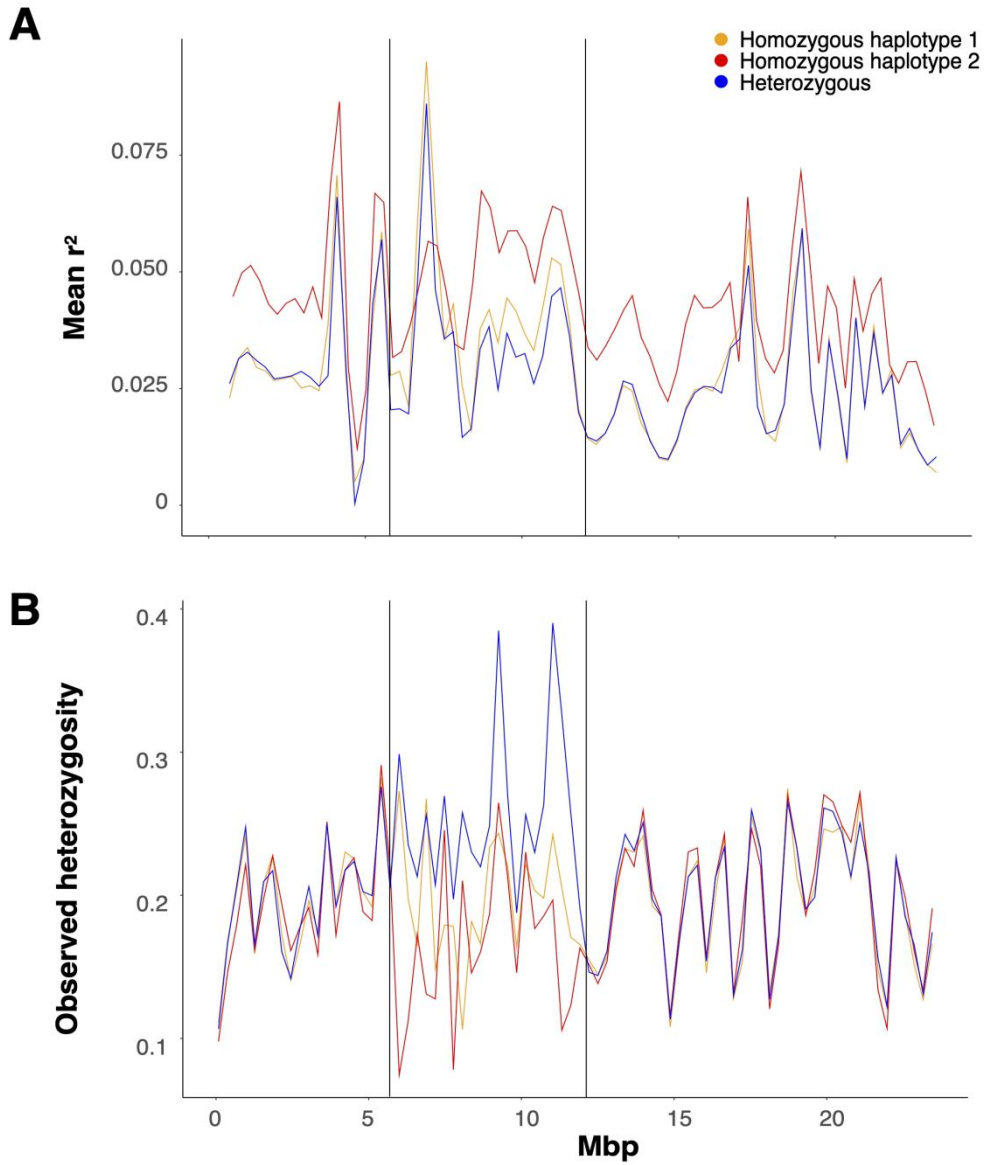


1  
2 664 **Supplementary Figure 7. Chromosome 15 haplotype clusters inferred from chromosome 15 PCA**  
3 665 **loadings on PC1.**



30 666

Supplementary Figure 8. Pearson's  $r^2$  correlation between LD ( $r^2$ ) of each SNP with 50 adjacent SNPs (A) and observed heterozygosity across chromosome S15, estimated separately within individuals homozygous or heterozygous for each haplotype.



## References

- Ali, O. A., O'Rourke, S. M., Amish, S. J., Meek, M. H., Luikart, G., Jeffres, C., and Miller, M. R. 2016. RAD capture (Rapture): Flexible and efficient sequence-based genotyping. *Genetics*, 202: 389–400.
- Andrews, S. (2010). FastQC: a quality control tool for high throughput sequence data. Available online at: <http://www.bioinformatics.babraham.ac.uk/projects/fastqc>
- Armsworthy, S. L., and Campana, S. E. 2010. Age determination, bomb-radiocarbon validation and growth of Atlantic halibut (*Hippoglossus hippoglossus*) from the Northwest Atlantic. *Environmental Biology of Fishes*, 89: 279–295
- Assis, J., Tyberghein, L., Bosch, S., Verbruggen, H., Serrão, E. A., and De Clerck, O. 2018. Bio-ORACLE v2.0: Extending marine data layers for bioclimatic modelling. *Global Ecology and Biogeography*, 27(3): 277–284.
- Babin, C., Gagnaire, P.A., Pavey, S.A. and Bernatchez, L. 2017. RAD-seq reveals patterns of additive polygenic variation caused by spatially-varying selection in the American eel (*Anguilla rostrata*). *Genome Biology and Evolution*. 9(11):2974-86
- Baird, N.A., Etter, P.D., Atwood, T.S., Currey, M.C., Shiver, A.L., Lewis, Z.A., Selker, E.U., Cresko, W.A., and Johnson, E.A. 2008. Rapid SNP discovery and genetic mapping using sequenced RAD markers. *PLoS ONE*, 3(10): e3376.
- Barbato, M., Orozco-terWengel, P., Tapio, M. and Bruford, M.W. 2015. SNeP: a tool to estimate trends in recent effective population size trajectories using genome-wide SNP data. *Frontiers in Genetics*, 6: 109.
- Bay, R.A., Rose, N., Barrett, R., Bernatchez, L., Ghalambor, C.K., Lasky, J.R., Brem, R.B., Palumbi, S.R., and Ralph, P. 2017. Predicting responses to contemporary environmental change using evolutionary response architectures. *The American Naturalist*. 189(5): 463-473.
- Bay, R.A. and Palumbi, S.R. 2014. Multilocus adaptation associated with heat resistance in reef-building corals. *Current Biology*. 24(24): 2952-2956.
- Benestan, L., Gosselin, T., Perrier, C., Sainte-Marie, B., Rochette, R., and Bernatchez, L. 2015. RAD genotyping reveals fine-scale genetic structuring and provides powerful population assignment in a widely distributed marine species, the American lobster (*Homarus americanus*). *Molecular Ecology*, 24(13): 3299-315.
- Benestan, L., Quinn, B.K., Maaroufi, H., Laporte, M., Clark, F.K., Greenwood, S.J., Rochette, R., and Bernatchez, L. 2016. Seascape genomics provides evidence for thermal adaptation and current-mediated population structure in American lobster (*Homarus americanus*). *Molecular Ecology*, 25:5073-5092.

- 1  
2 702 Berg, P.R., Jentoft, S., Star, B., Ring, K.H., Knutsen, H., Lien, S., Jakobsen, K.S., and Andre, C. 2015.  
3 703 Adaptation to low salinity promotes genomic divergence in Atlantic cod (*Gadus morhua* L.). *Genome*  
4 704 *Biology and Evolution*, 7(6): 1644-63.  
5 705
- 6 706 Bosch, S. 2018. sdmpredictors: Species distribution modelling predictor datasets. R package version  
7 707 0.2.8. Retrieved from <http://CRAN.R-project.org/package=sdmpredictors>  
8 708
- 9 709 Boudreau, S.A., Shackell, N.L., Carson, S., and den Heyer, C.E. 2017. Connectivity, persistence, and  
10 710 loss of high abundance areas of a recovering marine fish population in the Northwest Atlantic Ocean.  
11 711 *Ecology and Evolution*. 2017 7(22):9739-9749.  
12 712
- 13 713 Bradbury, I.R., Hubert, S., Higgins, B., Borza, T., Bowman, S., Paterson, I.G., Snelgrove, P.V., Morris,  
14 714 C.J., Gregory, R.S., Hardie, D.C., Hutchings, J.A., Ruzzante, D.E., Taggart, C.T., Bentzen, P. 2010.  
15 715 Parallel adaptive evolution of Atlantic cod on both sides of the Atlantic Ocean in response to  
16 716 temperature. *Proceedings of the Royal Society B: Biological Sciences*. 277(1701):3725-3734.  
17 717
- 18 718 Brennan, C.E., Blanchard, H., and Fennel, K. 2012. Putting temperature and oxygen thresholds of  
19 719 marine animals in context of environmental change: a regional perspective for the Scotian Shelf and  
20 720 Gulf of St. Lawrence. *PloS ONE*, 11(12): e0167411.  
21 721
- 22 722 Browning, S. R., and Browning, B.L. 2007. Rapid and accurate haplotype phasing and missing data  
23 723 inference for whole genome association studies by use of localized haplotype clustering. *American*  
24 724 *Journal of Human Genetics*, 81:1084-1097.  
25 725
- 26 726 Cáceres A., Sindi, S.S., Raphael, B.J., Cáceres, M., and González, J.R. 2012. Identification of  
27 727 polymorphic inversions from genotypes. *BMC Bioinformatics*, 13:28.  
28 728
- 29 729 Capblancq, T., Luu, K., Blum, M.G., and Bazin, E. 2018. Evaluation of redundancy analysis to identify  
30 730 signatures of local adaptation. *Molecular Ecology Resources*. 18(6):1223-1233.  
31 731
- 32 732 Carrier, E., Ferchaud, A.L., Normandeau, E., Sirois, P., and Bernatchez, L. 2020. Estimating the  
33 733 contribution of Greenland Halibut (*Reinhardtius hippoglossoides*) stocks to nurseries by means of  
34 734 Genotyping-By-Sequencing: sex and time matter. *Evolutionary Applications*,  
35 735 <https://doi.org/10.1111/eva.12979>  
36 736
- 37 737 Cayuela H., Rougemont, Q., Laporte, M., Mérot, C., Normandeau, E., Dorant, Y., Tørresen, O.K, Hoff,  
38 738 S.N., Jentoft, S., Sirois, P., Castonguay, M., [Jansen](#), T., Praebel, K., Clement, M., and Bernatchez, L.  
39 739 2020. Shared ancestral polymorphism and chromosomal rearrangements as potential drivers of local  
40 740 adaptation in a marine fish. *Molecular Ecology*. <https://doi.org/10.1111/mec.15499>  
41 741
- 42 742 Chang, C., Chow, C., Tellier, L., Vattikuti, S., Purcell, S. M., and Lee, J.J. 2015. Second-generation  
43 743 PLINK: Rising to the challenge of larger and richer datasets. *GigaScience*, 4, 7.  
44 744
- 45 745 Chen, S., Zhang, G., Shao, C., Huang, Q., Liu, G., Zhang, P., Song, W., An, N., Chalopin, D., Volff,  
46 746 J.N., and Hong, Y. 2014. Whole-genome sequence of a flatfish provides insights into ZW sex  
47 747 chromosome evolution and adaptation to a benthic lifestyle. *Nature Genetics*, 46: 253-260.  
48 748  
49 749  
50 750  
51 751  
52 752  
53 753  
54 754  
55 755  
56  
57  
58  
59  
60

- 1  
2 Cristofari, R., Liu, X., Bonadonna, F., Cherel, Y., Pistorius, P., Le Maho, Y., Raybaud, V., Stenseth,  
3 N.C., Le Bohec, C. and Trucchi E. 2018. Climate-driven range shifts of the king penguin in a  
4 fragmented ecosystem. *Nature Climate Change*. 8(3):245-51.  
5
- 6  
7 744 Danecek, P., Auton, A., Abecasis, G., Albers, C.A., Banks, E., DePristo, M.A., Handsaker, R.E.,  
8 745 Lunter, G., Marth, G.T., Sherry, S.T., and McVean, G. 2011. The variant call format and VCFtools.  
9 746 *Bioinformatics*, 27: 2156-2158.  
10 747
- 11 748 den Heyer, C. E., Armsworthy, A., Wilson, S., Wilson, G., Bajona, L., Bond, S., and Trzcinski, M. K.  
12 749 2012. Atlantic Halibut all-sizes tagging program summary report for 2006 to 2011. Canadian Technical  
13 750 Report of Fisheries and Aquatic Sciences, 2992, vi+38 p.  
14 751
- 15 752 Delrieu-Trottin, E., Hubert, N., Giles, E.C., Chifflet-Belle, P., Suwalski, A., Neglia, V.,  
16 753 Rapu-Edmunds, C., Mona, S., and Saenz-Agudelo, P. 2020. Coping with Pleistocene climatic  
17 754 fluctuations: Demographic responses in remote endemic reef fishes. *Molecular Ecology*, 29(12):2218-  
18 755 33.  
19 756
- 20 757 DePristo, M.A., Banks, E., Poplin, R., Garimella, K.V., Maguire, J.R., Hartl, C., Philippakis, A.A., Del  
21 758 Angel, G., Rivas, M.A., Hanna, M., McKenna, A. 2011. A framework for variation discovery and  
22 759 genotyping using next-generation DNA sequencing data. *Nature Genetics*, 43: 491-498.  
23 760
- 24 761 DFO. (2015a). 2014 Assessment of Atlantic Halibut on the Scotian Shelf and Southern Grand Banks  
25 762 (NAFO Divisions 3NOPs4VWX5Zc). DFO Canadian Science Advisory Secretariat Science Advisory  
26 763 Report, 2015/012.  
27 764
- 28 765 DFO. (2015b). Stock Assessment of Atlantic Halibut of the Gulf of St. Lawrence (NAFO Division  
29 766 4RST) for 2013 and 2014. DFO Canadian Science Advisory Secretariat Science Advisory Report,  
30 767 2015/023.  
31 768
- 32 769 DFO. (2018a). Atlantic Halibut. Ottawa, Ontario: Fisheries and Oceans Canada. Retrieved from  
33 770 <http://dfo-mpo.gc.ca/species-especes/profiles-profils/atl-halibut-fletan-atl-eng.html>
- 34 771 Do, C., Waples, R.S., Peel, D., Macbeth, G.M., Tillett, B.J., and Ovenden JR. 2014. NEESTIMATOR  
35 772 v2: re-implementation of software for the estimation of contemporary effective population size ( $N_e$ )  
36 773 from genetic data. *Molecular Ecology Resources*, 14: 209-214.  
37 774 Einfeldt, A.L., Kess, T., Messmer, A., Duffy, S., Wringe, B., Fisher, J., den Heyer, C., Shackell, N.,  
38 775 Bradbury, I.R., Ruzzante, D., and Bentzen, P. 2021. Chromosome level reference of Atlantic Halibut  
39 776 *Hippoglossus hippoglossus* provides insight into the evolution of sexual determination systems. *In*  
40 777 *review: Molecular Ecology Resources*, ID: MER-20-0424  
41 778  
42 779
- 43 780 Flaxman, S.M., Wacholder, A.C, Feder, J.L, and Nosil, P. 2014. Theoretical models of the influence of  
44 781 genomic architecture on the dynamics of speciation. *Molecular Ecology*, 23:4074-4088.  
45 782
- 46 783 Frichot, E. and Francois, O. 2015. LEA: An R Package for landscape and ecological association  
47 784 studies. *Methods in Ecology and Evolution*, 6: 925–929.  
48 785
- 49 786 Frichot, E., Mathieu, F., Trouillon, T., Bouchard, G., and François, O. 2014. Fast and efficient  
50 787 estimation of individual ancestry coefficients. *Genetics*, 196: 973–983.  
51 788  
52 789  
53 790  
54 791  
55 792  
56 793  
57 794  
58 795  
59 796  
60 797

- 1  
2 788  
3 789 Funk, W. C., McKay, J. K., Hohenlohe, P. A., and Allendorf, F. W. 2012. Harnessing genomics for  
4 790 delineating conservation units. *Trends in Ecology & Evolution*, 27: 489–496.  
5 791
- 6 792 Gagnaire, P. A., Broquet, T., Aurelle, D., Viard, F., Souissi, A., Bonhomme, F., Arnaud-Haond, S., and  
7 793 Bierne, N. 2015. Using neutral, selected, and hitchhiker loci to assess connectivity of marine  
8 794 populations in the genomic era. *Evolutionary Applications*, 8(8): 769-786.  
9 795
- 10 796 Gagnaire PA, Gaggiotti OE. Detecting polygenic selection in marine populations by combining  
11 797 population genomics and quantitative genetics approaches. *Current Zoology*. 2016 Dec 1;62(6):603-16.  
12 798
- 13 799 Gatti, P., Robert, D., Fisher, J.A., Marshall, R.C., and Le Bris, A. 2020. Stock-scale electronic tracking  
14 800 of Atlantic Halibut reveals summer site fidelity and winter mixing on common spawning grounds.  
15 801 *ICES Journal of Marine Science*. <https://doi.org/10.1093/icesjms/fsaa162>  
16 802
- 17 803 Grasso, G.M. 2008. What appeared limitless plenty: the rise and fall of the nineteenth-century Atlantic  
18 804 halibut fishery. *Environmental History*, 13(1): 66-91.  
19 805
- 20 806 Hauser, L., and Carvalho, G. R. 2008. Paradigm shifts in marine fisheries genetics: ugly hypotheses  
21 807 slain by beautiful facts. *Fish and Fisheries*: 9: 333-62.  
22 808
- 23 809 Healy, T.M., Brennan, R.S., Whitehead, A., and Schulte, P.M. 2018. Tolerance traits related to climate  
24 810 change resilience are independent and polygenic. *Global Change Biology*. 24(11):5348-5360.  
25 811
- 26 812 Hoegh-Guldberg, O., and Bruno, J.F. 2010. The impact of climate change on the world's marine  
27 813 ecosystems. *Science*, 328(5985):1523-1528.  
28 814
- 29 815 Hollenbeck, C.M., Portnoy, D.S. and Gold, J.R. 2016. A method for detecting recent changes in  
30 816 contemporary effective population size from linkage disequilibrium at linked and unlinked loci.  
31 817 *Heredity*, 117:207-216.  
32 818
- 33 819 Hooper, D. M., and Price, T. D. 2017. Chromosomal inversion differences correlate with range overlap  
34 820 in passerine birds. *Nature Ecology and Evolution*, 1: 1526–1534.  
35 821
- 36 822 Jiménez-Mena, B., Le Moan, A., Christensen, A., van Deurs, M., Mosegaard, H., Hemmer-Hansen, J.,  
37 823 and Bekkevold, D. 2020. Weak genetic structure despite strong genomic signal in lesser sand eel in the  
38 824 North Sea. *Evolutionary Applications*, 12:376-387.  
39 825
- 40 826 Kardos M, Taylor HR, Ellegren H, Luikart G, Allendorf FW. Genomics advances the study of  
41 827 inbreeding depression in the wild. *Evolutionary applications*. 2016 Dec;9(10):1205-18.  
42 828
- 43 829 Kelley, J.L., Brown, A.P., Therkildsen, N.O., Foote, and A.D. 2016. The life aquatic: advances in  
44 830 marine vertebrate genomics. *Nature Reviews Genetics*, 17:523-524.  
45 831
- 46 832 Kersula, M., and Seitz, A. Diverse migratory behaviors of Atlantic halibut (*Hippoglossus hippoglossus*,  
47 833 L.) based on the 2000–2017 Maine halibut tagging program. *Journal of Northwest Atlantic Fishery  
48 834 Science*, 50:13-24.  
49 835  
50 836  
51 837  
52 838  
53 839  
54 840  
55 841  
56 842  
57 843  
58 844  
59 845  
60 846

- 1  
2 831 Kess, T., Bentzen, P., Lehnert, S.J., Sylvester, E.V., Lien, S., Kent, M.P., Sinclair-Waters, M., Morris,  
3 832 C., Wringe, B., Fairweather, R., and Bradbury, I.R. 2020 Modular chromosome rearrangements reveal  
4 833 parallel and nonparallel adaptation in a marine fish. *Ecology and Evolution*, 10(2):638-53.  
5 834
- 6 835 Kess, T., Bentzen, P., Lehnert, S.J., Sylvester, E.V., Lien, S., Kent, M.P., Sinclair-Waters, M., Morris,  
7 836 C.J., Regular, P., Fairweather, R. and Bradbury, I.R. 2019. A migration-associated supergene reveals  
8 837 loss of biocomplexity in Atlantic cod. *Science advances*. 5(6):eaav2461.  
9 838
- 10 839 Korneliussen, T.S., Albrechtsen, A., and Nielsen, R. 2014. ANGSD: analysis of next generation  
12 840 sequencing data. *BMC Bioinformatics*, 15, 356.  
13 841
- 14 842 Layton, K.K.S., Snelgrove, P.V.R., Dempson, J.B., Kess, T., Lehnert, S.J., Bentzen, P., Duffy, S.J.,  
15 843 Messmer, A.M., Stanley, R.R.E., DiBacco, C., Salisbury, S.J., Ruzzante, D.E., Nugent, C.M.,  
16 844 Ferguson, M.M., Leong, J.S., Koop, B.F., and Bradbury, I.R. 2021. Past and future climate-linked loss  
17 845 in the most northerly freshwater fish. *Nature Climate Change (in press)*: doi.10.1038/s41558-020-  
18 846 00959-7.  
19 847
- 20 848 Lamichhaney, S., Barrio, A.M., Rafati, N., Sundström, G., Rubin, C.J., Gilbert, E.R., Berglund, J.,  
21 849 Wetterbom, A., Laikre, L., Webster, M.T., and Grabherr, M. 2012. Population-scale sequencing reveals  
22 850 genetic differentiation due to local adaptation in Atlantic herring. *Proceedings of the National Academy*  
23 851 *of Sciences*. 109(47): 19345-19350.  
24 852
- 25 853 Le Bris, A., Fisher, J.A., Murphy, H.M., Galbraith, P.S., Castonguay, M., Loher, T., and Robert, D.  
26 854 Migration patterns and putative spawning habitats of Atlantic halibut (*Hippoglossus hippoglossus*) in  
27 855 the Gulf of St. Lawrence revealed by geolocation of pop-up satellite archival tags. *ICES Journal of*  
28 856 *Marine Science*, 75:135-147.  
29 857
- 30 858 Le Corre, V. and Kremer, A. 2012. The genetic differentiation at quantitative trait loci under local  
31 859 adaptation. *Molecular Ecology*. 21(7):1548-66.  
32 860
- 33 861 Lehnert, S.J., Kess, T., Bentzen, P., Kent, M.P., Lien, S., Gilbey, J., Clément, M., Jeffery, N.W.,  
34 862 Waples, R.S. and Bradbury, I.R.. 2019. Genomic signatures and correlates of widespread population  
35 863 declines in salmon. *Nature Communications*, 10: 2996.  
36 864
- 37 864 Li, H. 2013. Aligning sequence reads, clone sequences and assembly contigs with BWA-MEM. *ArXiv*,  
38 865 1303, 3997.  
39 866
- 40 867 Li, H., Handsaker, B., Wysoker, A., Fennell, T., Ruan, J., Homer, N., Marth, G., Abecasis, G., and  
41 868 Durbin, R. 2009. The sequence alignment/map format and SAMtools. *Bioinformatics*, 25(16): 2078-  
42 869 2079.  
43 870
- 44 870 Liu, X. and Fu, Y.X. 2015. Exploring population size changes using SNP frequency spectra. *Nature*  
45 871 *Genetics*, 47(5): 555-559.  
46 872
- 47 873 Liu, X., and Fu, Y.X. 2020. Stairway Plot 2: demographic history inference with folded SNP frequency  
48 874 spectra. *Genome Biology* 21, 280. <https://doi.org/10.1186/s13059-020-02196-9>  
49 875  
50 876  
51 877  
52 878  
53 879  
54 880  
55 881  
56 882  
57 883  
58 884  
59 885  
60 886



- 1  
2 Longo, G.C., Lam, L., Basnett, B., Samhouri, J., Hamilton, S., Andrews, K., Williams, G., Goetz, G.,  
3 McClure, M., and Nichols, K.M. 2020. Strong population differentiation in Lingcod (*Ophiodon*  
4 *elongatus*) is driven by a small portion of the genome. *Evolutionary Applications*, 13(10):2536-54.  
5
- 6  
7 871 Lotterhos, K.E. 2019. The effect of neutral recombination variation on genome scans for selection. *G3:*  
8 872 *Genes, Genomes, Genetics*. 9(6):1851-1867.  
9 873
- 10 874 Luu, K., Bazin, E., and Blum, M.G.B. 2017. pcadapt: An R package for performing genome scans for  
11 875 selection based on principal component analysis. *Molecular Ecology Resources*, 17, 67–77.  
12 876
- 13 877 Marçais G, Delcher AL, Phillippy AM, Coston R, Salzberg SL, Zimin A. 2018. MUMmer4: a fast and  
14 878 versatile genome alignment system. *PLoS Computational Biology*, 14(1): e1005944.  
15 879
- 16 880 Martin, M. (2011) Cutadapt removes adapter sequences from high-throughput sequencing reads.  
17 881 *EMBnet. Journal*, 17(1),10-12.  
18 882  
19 883  
20 884
- 21  
22  
23 Mazet, O., Rodríguez, W., Grusea, S., Boitard, S., and Chikhi, L. 2016. On the importance of being  
24 structured: instantaneous coalescence rates and human evolution—lessons for ancestral population size  
25 inference? *Heredity*, 116(4):362-371.  
26
- 27 Mérot C., Oomen, R.A., Tigano, A., and Wellenreuther, M. 2020. A roadmap for understanding the  
28 evolutionary significance of structural genomic variation. *Trends in Ecology & Evolution*, 35(7):561-  
29 572.  
30
- 31 885  
32 886 Mi, H., Muruganujan, A., Huang, X., Ebert, D., Mills, C., Guo, X., and Thomas, P.D. 2019. Protocol  
33 887 Update for large-scale genome and gene function analysis with the PANTHER classification system (v.  
34 888 14.0). *Nature Protocols*. 14: 703-21.  
35 889
- 36 890 Mitchell-Olds, T., Willis, J.H. and Goldstein, D.B. 2007. Which evolutionary processes influence  
37 891 natural genetic variation for phenotypic traits? *Nature Reviews Genetics*, 8: 845–856.  
38 892
- 39 893 Nielsen, J.G. 1986. Pleuronectidae. 1299-1307. *Fishes of the North-eastern Atlantic and the*  
40 894 *Mediterranean*. UNESCO, Paris. Vol. 3.  
41 895  
42 896  
43
- 44 896 Oksanen, J., Blanchet, F.G., Kindt, R., Legendre, P., O'hara, R.B., Simpson, G.L., Solymos, P.,  
45 897 Stevens, M.H., and Wagner, H. 2011 vegan: community ecology package. R package version 1.17-4.  
46 898 URL <http://CRAN.R-project.org/package=vegan>.  
47 899
- 48 900 Pearse, D.E., Barson, N.J., Nome, T., Gao, G., Campbell, M.A., Abadía-Cardoso, A., Anderson, E.C.,  
49 901 Rundio, D.E., Williams, T.H., Naish, K.A., Moen T *et al.* 2019. Sex-dependent dominance maintains  
50 902 migration supergene in rainbow trout. *Nature Ecology & Evolution*, 3:1731-1742.  
51 903  
52 904
- 53 904 Pembleton, L.W., Cogan, N.O., and Forster, J.W. 2013. StAMPP: An R package for calculation of  
54 905 genetic differentiation and structure of mixed-ploidy level populations. *Molecular Ecology Resources*,  
55 906 13(5):946-952.  
56 907  
57 908  
58  
59  
60

- 1  
2 908 Pespeni, M.H., and Palumbi, S.R. 2013. Signals of selection in outlier loci in a widely dispersing  
3 909 species across an environmental mosaic. *Molecular Ecology*, 22(13):3580-3597.  
4 910
- 5 Prince, D.J., O'Rourke, S.M., Thompson, T.Q., Ali, O.A., Lyman, H.S., Saglam, I.K., Hotaling, T.J.,  
6 Spidle, A.P., and Miller, M.R. 2017. The evolutionary basis of premature migration in Pacific salmon  
7 highlights the utility of genomics for informing conservation. *Science Advances*. 3(8): e1603198.  
8  
9
- 10 911 Quinlan, A.R., and Hall I.M. 2010. BEDTools: a flexible suite of utilities for comparing genomic  
11 912 features. *Bioinformatics*, 26; 841-842.
- 12 913 Rao, C. R. 1964. The use and interpretation of principal component analysis in applied research.  
13 914 *Sankhya: The Indian Journal of Statistics, Series A*, 26: 329–358.
- 14 915 Reid, D.P., Pongsomboon, S., Jackson, T., McGowan, C., Murphy, C., Martin-Robichaud, D., and  
15 916 Reith, M. 2005. Microsatellite analysis indicates an absence of population structure among  
16 917 *Hippoglossus hippoglossus* in the north-west Atlantic. *Journal of Fish Biology* 67(2):570-6.  
17 918
- 18 919 Reid, D.P., Smith, C.A., Rommens, M., Blanchard, B., Martin-Robichaud, D., and Reith M. 2007. A  
19 920 genetic linkage map of Atlantic Halibut (*Hippoglossus hippoglossus* L.). *Genetics*. 177(2):1193-1205.  
20 921
- 21 922 Rey, C., Darnaude, A., Ferraton, F., Guinand, B., Bonhomme, F., Bierne, N., and Gagnaire, P.A. 2020.  
22 923 Within-generation polygenic selection shapes fitness-related traits across environments in juvenile sea  
23 924 bream. *Genes*. 2020 11(4):398.  
24 925
- 25 926 Rochette, N.C., Rivera-Colón, A.G., and Catchen, J.M. 2019. Stacks 2: Analytical methods for  
26 927 paired-end sequencing improve RADseq-based population genomics. *Molecular Ecology*, 28(21):  
27 928 4737-4754.  
28 929
- 29 930 Ruzzante, D.E., Walde, S. J., Gosse, J. C., Cussac, V. E., Habit, E., Zemplak, T.S., and Adams, E. D. M.  
30 931 2008. Climate control on ancestral population dynamics: Insight from Patagonian fish phylogeography.  
31 932 *Molecular Ecology* 17: 2234 - 2244.  
32 933
- 33 934 \
- 34 935 Savolainen, O., Lascoux, M., and Merilä, J. 2013. Ecological genomics of local adaptation. *Nature*  
35 936 *Reviews Genetics*, 14:807-20.  
36 937
- 37 938 Selkoe, K.A., Aloia, C.C., Crandall, E.D., Iacchei, M., Liggins, L., Puritz, J.B., von der Heyden, S., and  
38 939 Toonen, R.J. 2016. A decade of seascape genetics: contributions to basic and applied marine  
39 940 connectivity. *Marine Ecology Progress Series*, 554:1-19.
- 40 941 Shackell, N.L., Bundy, A., Nye, J.A., and Link, J.S. 2012. Common large-scale responses to climate  
41 942 and fishing across Northwest Atlantic ecosystems. *ICES Journal of Marine Science*, 69(2):151-62.  
42 943
- 43 944 Shackell, N.L., Ferguson, K.J., den Heyer, C.E., Brickman, D., Wang, Z., and Ransier, K.T. 2019.  
44 945 Growing degree-day influences growth rate and length of maturity of Northwest Atlantic halibut  
45 946 (*Hippoglossus hippoglossus* L.) across the southern stock domain. *Journal of Northwest Atlantic*  
46 947 *Fishery Science*,50:25-35.  
47 948
- 48 949 Shackell, N.L., Frank, K.T., Nye, J.A., and den Heyer, C.E.. 2016. A transboundary dilemma:  
49 950 dichotomous designations of Atlantic halibut status in the Northwest Atlantic. *ICES Journal of Marine*  
50 951 *Science*, 73(7):1798-805.  
51 952  
52 953  
53 954  
54 955  
55 956  
56 957  
57 958  
58 959  
59 960

1  
2  
3 Stanley, R.R., DiBacco, C., Lowen, B., Beiko, R.G., Jeffery, N.W., Van Wyngaarden, M., Bentzen, P.,  
4 Brickman, D., Benestan, L., Bernatchez, L., Johnson, C. Snelgrove, P.V.R., Wang, Z., Wringe, B.F.  
5 and Bradbury, I.R. 2018. A climate-associated multispecies cryptic cline in the northwest Atlantic.  
6 Science Advances, 4(3):eaaq0929.  
7

939

940

10 941 Stevens, E.L., Heckenberg, G., Roberson, E.D., Baugher, J.D., Downey, T.J., and Pevsner, J. 2011.  
11 942 Inference of relationships in population data using identity-by-descent and identity-by-state. PLoS  
12 943 Genetics, 7(9):e1002287.  
13

944

14 945 Stobo, W.T., Neilson, J.D., and Simpson, P.G. 1988. Movements of Atlantic halibut (*Hippoglossus*  
15 946 *hippoglossus*) in the Canadian North Atlantic. Canadian Journal of Fisheries and Aquatic Sciences,  
16 947 45(3):484-491.  
17

948

18 949 Storey, J.D., Bass, A.J., Dabney, A., and Robinson, D. 2015. qvalue: Q-value estimation for false  
19 950 discovery rate control. R package version 2.10.0.<http://github.com/jdstorey/qvalue>  
20

951

21 952 Storey J.D., and Tibshirani, R. (2003) Statistical significance for genome-wide studies. Proceedings of  
22 953 the National Academy of Sciences of the United States of America, 100: 9440–9445.  
23

954

24 955 Supek, F., Bošnjak, M., Škunca, N., and Šmuc, T. 2011. REVIGO summarizes and visualizes long lists  
25 956 of gene ontology terms. PloS ONE.6(7): e21800.  
26

957

27 958 Thompson, M., and Jiggins, C. 2014. Supergenes and their role in evolution. Heredity, **113**: 1–8  
28

959

29 960 Trzcinski, M.K., and Bowen, W.D. 2016. The recovery of Atlantic halibut: a large, long-lived, and  
30 961 exploited marine predator. ICES Journal of Marine Science. 73(4): 1104-1114.  
31

962

32 963 Van Wyngaarden, M., Snelgrove, P.V., DiBacco, C., Hamilton, L.C., Rodríguez-Ezpeleta, N., Jeffery,  
33 964 N. W., Stanley, R. R., and Bradburym I. R. 2017. Identifying patterns of dispersal, connectivity and  
34 965 selection in the sea scallop, *Placopecten magellanicus*, using RAD seq-derived SNP s. Evolutionary  
35 966 Applications, 10(1) :102-17.  
36

967

37 968 Vijay, N., Park, C., Oh, J., Jin, S., Kern, E., Kim, H.W., Zhang, J., and Park, J.K. 2018. Population  
38 969 genomic analysis reveals contrasting demographic changes of two closely related dolphin species in the  
39 970 last glacial. Molecular Biology and Evolution, 35(8):2026-33.  
40

971

41 972 Waples, R.S. and Lindley, S.T. 2018. Genomics and conservation units: The genetic basis of adult  
42 973 migration timing in Pacific salmonids. Evolutionary Applications. 11(9):1518-26.  
43

974

44 975 Weir, B.S., and Cockerham, C.C. 1984. Estimating F-statistics for the analysis of population structure.  
45 976 Evolution, 38: 1358–1370.  
46

977

47 978 Wang, L., Beissinger, T.M., Lorant, A., Ross-Ibarra, C., Ross-Ibarra, J. and Hufford, M.B. 2017. The  
48 979 interplay of demography and selection during maize domestication and expansion. Genome Biology,  
49 980 18:215.  
50

981

982

983

984

985

1  
2 977 Xuereb, A., Kimber, C.M., Curtis, J.M., Bernatchez, L., and Fortin, M.J. 2018. Putatively adaptive  
3 978 genetic variation in the giant California sea cucumber (*Parastichopus californicus*) as revealed by  
4 979 environmental association analysis of restriction-site associated DNA sequencing data. *Molecular*  
5 980 *Ecology*, 27: 5035-5048.  
6  
7 981  
8 982  
9 983  
10 984  
11 985  
12 986  
13 987  
14 988  
15 989  
16 990  
17 991  
18 992  
19 993  
20 994  
21 995  
22 996  
23 997  
24 998  
25 999  
26 1000  
27 1001  
28 1002  
29 1003  
30 1004  
31 1005  
32  
33  
34  
35  
36  
37  
38  
39  
40  
41  
42  
43  
44  
45  
46  
47  
48  
49  
50  
51  
52  
53  
54  
55  
56  
57  
58  
59  
60

For Review Only